



HAL
open science

In-depth exploration of defects in zeolite membranes: Typology, formation, characterization and healing

Fatima Zohra Charik, Brahim Achiou, Abdessamad Belgada, Mohamed Ouammou, Murielle Rabiller-Baudry, Saad Alami Younssi

► To cite this version:

Fatima Zohra Charik, Brahim Achiou, Abdessamad Belgada, Mohamed Ouammou, Murielle Rabiller-Baudry, et al.. In-depth exploration of defects in zeolite membranes: Typology, formation, characterization and healing. *Journal of Environmental Chemical Engineering*, 2024, 12 (3), pp.112918. 10.1016/j.jece.2024.112918 . hal-04615596

HAL Id: hal-04615596

<https://hal.science/hal-04615596v1>

Submitted on 2 Jul 2024

HAL is a multi-disciplinary open access archive for the deposit and dissemination of scientific research documents, whether they are published or not. The documents may come from teaching and research institutions in France or abroad, or from public or private research centers.

L'archive ouverte pluridisciplinaire **HAL**, est destinée au dépôt et à la diffusion de documents scientifiques de niveau recherche, publiés ou non, émanant des établissements d'enseignement et de recherche français ou étrangers, des laboratoires publics ou privés.



Distributed under a Creative Commons Attribution - NonCommercial 4.0 International License

In-depth exploration of defects in zeolite membranes: typology, formation, characterization and healing

Fatima Zohra Charik ^{1,2,*}, Brahim Achiou ^{1,3,*}, Abdessamad Belgada ¹,

Mohamed Ouammou ¹, Murielle Rabiller-Baudry ², Saad Alami Younssi ¹,

¹ Faculty of Sciences and Techniques of Mohammedia, Hassan II University of Casablanca,

Morocco

² Univ Rennes, CNRS, (Institut des Sciences Chimiques de Rennes) - UMR- 6226, F-35000

Rennes France

³ Institute of Science, Technology & Innovation (IST&I), Mohammed VI Polytechnic

University (UM6P), Ben Guerir, 43150, Morocco

*Corresponding authors: fatimazohra.charik-etu@etu.univh2c.ma (F. Z. Charik);

brahim.achiou@fstm.ac.ma (B. Achiou)

Abstract

Unlocking the potential of zeolite membranes consists in overcoming the persistent challenge of defects formation, a barrier against their application at industrial scale. Understanding the mechanisms underlying defect formation is mandatory for achieving precise control and optimization of membrane performance. This paper offers a comprehensive exploration of the diverse defects of zeolite membranes, investigating the factors responsible for their occurrence during membrane preparation such as crystallization kinetics, seeding techniques and template removal. Furthermore, a variety of characterization techniques used to identify defects are examined, highlighting their features and drawbacks. This review also explores the current strategies to heal defects, including post-treatment methods and preparation optimization. Through this elucidation, the paper aims to make a progress in addressing the defect issue in zeolite membrane.

Keywords: Zeolite membrane; zeolite synthesis; defect; non-zeolitic pores; cracks; pinholes; grain boundaries.

1. Introduction

Zeolites are generally described as microporous crystalline aluminosilicates formed by the arrangement of TO_4 tetrahedra where T can generally be Si and Al atoms or in some cases: Ga, Ba, Ge, etc [1,2]. In light of their outstanding properties such as (i) ordered pore size, (ii) well-defined structure and (iii) molecular-sized microchannels, zeolites materials are widely explored in industry for different applications, including separation, ion-exchange, adsorption, sensing and catalysis [3–6]. Furthermore, there has been a growing interest in the use of zeolitic materials to fabricate zeolitic membranes. This is mainly due to their high thermal resistance and mechanical strength, good chemical stability, and long-life performance compared to organic membranes [1,4,7–9]. Zeolite membranes have been extensively used for gas separation, dehydration of solvents, organics separation and pervaporative desalination [10,11]. Up to now, more than 240 types of zeolites have been classified based on their specific framework structure as reported by the International Zeolite Association (IZA) [2]. However, few types of structures have been used in the preparation of zeolite membranes like faujasite (FAU) [12], chabazite (CHA) [13,14], mordenite (MOR) [15], mobil-five (MFI) [16], lindenmeyerite (LTA) [17–19], deca-dodecasil 3R (DDR) [20] and sodalite (SOD) [3].

Despite the great attention that zeolite membranes have received, there are still some challenging issues faced during membrane preparation notably reproducibility and occurrence of defects [21], which are the reason behind the only few existing large-scale zeolite membranes limited to dehydration of solvents [1]. Generally, defects are likely to form throughout the whole preparation process of zeolite membrane because of numerous factors such as synthesis method, nature/purity of precursors and seeding technique, as well as some specific applications like acid dehydration. For this reason, it is highly required to completely eliminate or treat these defects to maintain the high membrane performance [22].

In recent years, only few reviews targeting especially defects in zeolite membranes were published compared to the number of research papers about the preparation of zeolite membranes (**Fig. 1**). For example, *Maghsoudi et al.* reviewed the characterization techniques of defects in zeolite membranes, and studied the different methods for defects reparation [23]. *Xu et al.* presented a mini-review about the role of synthesis parameters in controlling the final features of prepared SAPO-34 zeolite membranes [24]. *Medeiros- costa et al.* focused in their review on silanol defects in the micropore structure of zeolites. They reported various techniques used for characterization and quantification of silanol-based defects. Furthermore, healing methods of silanol defects were also highlighted with a specific interest on the influence of the reparation techniques on properties of zeolites after treatment [25]. These reviews focused specifically on characterization and healing methods of defects in zeolite membranes [23], or discussed specific defects such as silanol-based defects [25]. Nevertheless, the elucidation of various kinds of defects that could exist in zeolite membranes has not been reported yet. Moreover, there is a lack of classification of defects and the explanation of different origins of their formation. To the best of our knowledge, no review has investigated the classification of various types of defects and the mechanism of their appearance. Thus, there is an immediate need to fill this knowledge gap in order to provide a deep insight into the different factors leading the formation of defects and profiling their types.

Accordingly, the purpose of this review is to give a full description of potential types of defects in zeolite membranes, beside their classification and formation mechanisms. Firstly, a classification of different types of defects was given, distinguishing between defects in zeolite materials and in membranes. Secondly, characterization techniques of these defects were summarized highlighting their advantages and inconveniences. More importantly, an entire discussion of factors leading to formation of defects were profoundly studied and explained. Finally, healing methods of defects have been also reviewed.

Fig. 1. Number of publications using the following keywords: (i) zeolite; membrane (marked with blue) and (ii) zeolite; membrane; defect (marked with green) (The data extracted from www.scopus.com).

2. Understanding of defects in zeolitic membranes

Generally, defects in zeolite materials are classified into four categories (**Fig. 2**), namely point defects, linear defects, two-dimensional defects and volume defects [26–29]. For zeolite materials, point defects are local imperfections related to the position of atoms *i.e.*, either presence of vacancies or impurities. For instance, a vacancy could result from Al atom removal from the framework, while an impurity could take the form of the presence of an atom different from that of the original structure [30]. Linear defects generally occur as dislocations defined as misaligned atoms in the interior of zeolite crystal [31]. Two-dimensional defects also known as planar defects are usually found on surfaces or interfaces like discontinuity in material. Volume defects could take the form of voids and grain boundaries. The exploration of different defect types is categorized into two primary classifications: defects within the zeolite crystal and defects within the membrane. These categories are interdependent, as imperfections within the zeolite crystal can manifest as flaws within the zeolite layer.

Fig. 2. Types of defects in zeolite materials and membranes.

2.1. Defects occurring in the zeolite crystal

Defects in the zeolite crystal manifest as disorders in the crystalline structure and may also include intracrystalline defects, which are known as silanols, resulting from unbalanced charges in the zeolite framework structure. They might also be present on the external surface of zeolite crystals, completing the valence of oxygen atoms. In general, silanols exist in the form of:

- Broken T-O-T bonds where T is Si or Al atoms like broken Si-O-Si bonds [32];
- Silanol nest formed where a T atom is missing, which means that the silanol nest surrounds a T vacancy. For instance, a tetrahedral Si atom is substituted with four

oxygen atoms linked to four hydrogen atoms [33], including either $(\text{HO-Si}\equiv)_4$ or $(\text{HO-Si}\equiv)_3$ (O^- -Si \equiv) groups [34].

Silanol groups (-OH) are generally formed by dealumination, which could take place either during the process of synthesis or during the application depending on the media conditions [35]. Dealumination consists in Al release from the framework of the zeolite because of steaming, calcination and acid leaching [36]. When the zeolite framework is exposed to water vapor at high temperatures (above 500 °C), Al-O-Si bonds are broken, and then silanol groups are formed in the edges of Si-O-Si network where oxygen atom is not linked to another Si atom [34]. On the other hand, it was evidenced that in contact with concentrated acids like nitric and acetic acids, Al-O-Si bonds are hydrolyzed leading to the formation of silanol groups [35]. Similarly, desilication causes the appearance of the same type of defect as dealumination [37]. This process lies in the release of silicon atom from a zeolite structure using alkaline treatment such as NaOH solution [38]. **Fig. 3** illustrates structural defects formed because of desilication. The leaching of zeolite crystals is also considered a form of defect where the structure of the crystal is damaged [39]. The dissolution of crystals depends on Al content in the framework structure. It was proven that the dissolution of zeolite diminishes with the presence of Al rich sites. At high pH during synthesis process, Al-rich sites are protected from hydroxide ion attack due to the negative charge. As a consequence, zeolites with a low Si/Al ratio are protected from this type of defects. **Fig. 4** shows the effect of alkaline treatment on the leaching of MFI zeolite.

Fig. 3. Structural defects throughout zeolite crystal [38].

Fig. 4. MFI zeolite (a) before and (b,c,d) after the alkaline treatment [39].

2.2. Defects occurring in the zeolite membrane layer

Defects in the zeolite membrane are identified to be pathways located near zeolite crystals and are larger in size compared to zeolite pores [40]. According to the International Union of Pure and Applied Chemistry (IUPAC), there are three types of zeolite membrane defects, including

macropore defects that have a size larger than 50 nm, mesopore defects that have a size range comprised between 2 and 50 nm, and micropore defects that have a size smaller than 2 nm [23]. Macropore defects are generally found in the form of cracks and pinholes. Cracks occur because of the thermal expansion that zeolite crystals undergo, and the shrinkage or expansion of membrane support [41]. It is noteworthy that zeolite materials have a negative coefficient of thermal expansion. However, for most commonly used ceramic supports, the coefficient of thermal expansion is positive, like for alumina substrates [42]. Mesopore and micropore defects are generated during the synthesis process due to defective intergrowth between zeolite crystals. This type of defect takes the form of intercrystalline pores that are present between the grains (i.e., open grain boundaries) [43]. Defects in zeolitic membranes are further detailed in **Section 4**.

3. Characterization techniques of defects

The performance of zeolite membranes depends on the type, number and size of defects. For this reason, it is extremely important to develop characterization techniques to quantify all defects of prepared membranes in order to evaluate their performance as selective layers. Two characterization approaches have been adopted to identify defects in zeolite membranes, notably direct and indirect techniques. Direct techniques give a visual observation of defects and mainly include microscopic techniques like scanning electron microscopy (SEM), while indirect techniques are based on the analysis of experimental data of species permeance that gives information about the number and size of defects.

3.1. Direct techniques

3.1.1. Scanning Electron Microscopy (SEM)

SEM is usually used to observe pinholes, cracks and grain boundaries defects. **Fig. 5** shows examples of SEM images of cracks defects that have taken place in different membranes,

including zeolite beta, NaY, and zeolite-Pd membranes. Generally, two forms of cracks can be distinguished, namely continuous and discontinuous cracks. Continuous cracks go from the membrane support to the zeolite layer and are known for cutting the membrane into pieces. Moreover, because of their larger size, these cracks have a negative significant impact on the membrane selectivity. Whist, discontinuous cracks occur only at the level of zeolite crystal as shown in **Fig. 5c**. **Fig. 6** displays a pinhole defect found in NaA zeolite membrane. The pinhole refers to a region on the zeolite layer's surface in which zeolite seeds were pierced into the support's pores under the vacuum force. It is worthy to note the difference between pinholes and a discontinuous zeolite layer. This latter results from the non-continuous seeding of the zeolite layer before crystallization. Conversely, a continuous seeded layer can induce pinholes after membrane preparation. SEM images in **Fig. 7** show grain boundaries caused by the size of seeds. Usually, seeds with larger grains lead to the formation of defective zeolite layers. It should be mentioned that the main limitation of the SEM technique is that it only allows the visualization of surface defects. However, it can also be employed to characterize volume defects carrying out SEM cross-views, but it is still not evident enough to provide accurate information about the defect.

Fig. 5. Cracks defects on the surface of (a) zeolite beta membrane (b) NaY zeolite membrane and (c) zeolite-Pd membrane [44–46].

Fig. 6. Pinholes defects on NaA zeolite membrane prepared from varyied concentration of seed solution (a) 0.5 wt% (b) 1 wt% (c) 2 wt% [47].

Fig. 7. (a) Top-view and (b) cross-view of grain boundaries defects on NaA zeolite membrane [47].

3.1.2. Fluorescence confocal optical microscopy (FCOM)

FCOM technique enables direct inspection and three-dimensional visualization of open grain boundaries, and sometimes for cracks identification. FCOM is based on the analysis of a dye

that passes through defects in a zeolite membrane. It should be mentioned that the choice of the fluorescent molecule is crucial; it should easily pass through defects. Therefore, the fluorescent molecule must be smaller in size than inter-crystalline defects. The FCOM images are interpreted as follows: the bright spot in the image means the presence of dye molecules, which refers to defects, and the dark surface indicates defect-free parts [48]. *Lee et al.* used FCOM technique to localize grain boundaries in MFI zeolite membrane [48]. It was reported that the contact time between the membrane and the dye solution plays a high role in screening defects. The longer the contact time is, more defects appear clearly in images. From **Fig. 8**, it can be seen that only a few bright spots showed up at a contact time of 7 days, however, when the time was increased to 15 days, the images became brighter suggesting that the dye solution further diffused to all grain boundaries existing in the zeolite layer. *Hong et al.* reported the characterization of cracks and grain boundaries in MFI zeolite membrane using sodium salt of fluorescein $C_{20}H_{10}Na_2O_5$ as a dye having a size of approximately 1 nm [49]. Cracks were easily observed after 2 days of dying (**Fig. 9b2-b3**) in contrast to grain boundaries that took 8 days to completely appear (**Fig. 9d1-d3**). These findings suggest that dye solution easily accumulates in cracks because their size is greater than that of grain boundaries. Cracks occurred in the middle of the MFI zeolite membrane (**Fig. 9c2,c3**), while grain boundaries were found at the membrane thickness, starting from the zeolite layer to the interface between the support and the membrane. The FCOM technique is considered non-destructive method [50], but it is restricted to the analysis of thick membranes because of the limited resolution of images [23]. When FCOM is utilized to characterize thin membranes, the concentration of dye should be reduced compared to that used for thicker membranes, in order to obtain accurate data and avoid interferences during analysis.

Fig. 8. FCOM images of MFI zeolite membrane in contact with dye molecules for (a) 7 days and (f) 15 days 10 μm [48].

Fig. 9. FCOM images of defects in MFI membrane (b2,b3) cracks at 2 days of dyeing (indicated by red and yellow lines), (c2,c3) grain boundaries at 4 days of dyeing (indicated by white circles) and (d2,d3) grain boundaries at 8 days of dyeing. The scale is 10 μm for all images [49].

3.2. Indirect techniques

3.2.1. Gas permeation

Gas permeation is based on the measurement of the ratio of single gas permeance of species. This method involves selecting two compounds: (i) small molecule that is allowed to diffuse faster in the zeolitic pore, and (ii) molecule with a larger size that is excluded. To provide information about the size of defects, researchers have used theoretical models that are established based on diffusion mechanisms. Generally, the transport of gas in zeolite pores is governed by surface diffusion or Knudsen diffusion. Surface diffusion includes three steps notably adsorption, diffusion and desorption [23]. While, Knudsen diffusion describes the transport of gas molecules by means of collisions with pore walls. The permeance of species through defects is also governed by Knudsen, but it can also occur by viscous flow or a combination of the two mechanisms [51]. Viscous flow takes place when gas molecules are struck by other gas molecules instead of the inner surface of pores [51]. Gas permeation relies on the fact that before calcination, gas molecules permeate through defects by means of Knudsen and viscous flow mechanisms as long as the zeolite pores are blocked with the organic template used for membrane synthesis. After calcination, gas molecules transfer through activated zeolite pores after the organic template removal following Knudsen mechanism. *Sorenson et al.* measured the ratio of single gas permeation of $\text{H}_2/\text{i-CH}_4$, $\text{N}_2/\text{i-CH}_4$, and $\text{H}_2/\text{i-CH}_4$ to evidence the existence of defects in NaA zeolite membrane [52]. i-CH_4 is selected due

to its larger kinetic diameter than NaA zeolite pores, which means that the permeation of *i*-CH₄ is primarily taking place through defects. It was reported that the transport of gas molecules is due to Knudsen diffusion. The number of defects was determined from the Knudsen diffusion ratio given by **Eq. (1)**. The He/*i*-CH₄ ratio was found to be 3.8, which means that the flux of He is 3.8 times higher than *i*-CH₄ flux. The He/*i*-CH₄ ratio of the membrane is 4.5, which results in a flux of He through defects of 84%. [52].

$$\alpha^{\circ}(i_1/i_2, k) = \sqrt{\frac{M(w, i_2)}{M(w, i_1)}} \quad (1)$$

Noting that $M(w, i_1)$ and $M(w, i_2)$ are molecular weights of gas i_1 and i_2 , respectively.

In another work, defects in DDR zeolite membrane were assessed using the single gas permeation ratio of $H_{2/i}$, where *i* is He, CH₄, N₂, O₂, CO₂ and *i*-C₄H₁₀. The obtained values were compared to the Knudsen factor. It was found that the theoretical values calculated from **Eq. (1)** are close to the ratio of single gas permeation suggesting the presence of large defects [53]. It is noteworthy that gas permeation technique is not useful for membranes that contain a lower number of defects because it is unable to detect small variations in gas permeation.

3.2.2. Permporosimetry

Permporosimetry technique is employed to quantify the number of defects via the measurement of He permeance through zeolite membrane. The concept of this technique is based on the use of a condensable component called adsorbate, which blocks zeolite pores while allowing a non-condensable gas (He) to permeate only through defects [23]. Permporosimetry data thus provide the percentage of He permeance through defects. *Qu et al.* applied this technique to evidence the existence of defects in NaA zeolite membrane, using He as the non-condensable gas and alcohols (ethanol, methanol and isopropanol) as adsorbates [54]. Adsorbate vapor was added to He in the feed, and the He permeance was measured while varying the adsorbate activity. It was concluded that as adsorbate activity increases, He permeance decreases. When using isopropanol, it was adsorbed into defects rather than into zeolite pores, because its size (0.48

nm) exceeds that of NaA zeolite pores. For ethanol, which has a size close to that of zeolite pores, a small amount is adsorbed resulting in the expansion of NaA zeolite crystals leading to the reduction of the size of defects, and hence decreasing the permeance of He. The same behavior was observed for methanol, which has a pore size smaller than NaA zeolite pore and is completely adsorbed, resulting in a significant decrease in permeance. It can be concluded that the choice of the condensable component is extremely important because it could affect defect characterization; thus it is recommended to select a component that does not swell zeolite crystals. In this context, *Lee et al.* obtained different results when characterizing defects in MFI zeolite membrane using benzene and *n*-hexane. When using benzene, it was found that 9% of the He flux passes through defects, whereas only 4.5% of the He flux was detected with the use of *n*-hexane. These results were explained by the expansion of MFI zeolite because of the presence of *n*-hexane and consequently reducing the size defects. Therefore, benzene is considered as a good candidate to characterize MFI zeolite membrane using permoporosimetry technique [55]. Another work reported the use of *n*-hexane/He to quantify defects in MFI zeolite membrane [56]. Experiments revealed that the He permeance through defects constituted 10% of the total He permeance. It was also found that defects represent 0.19% of the total area of the membrane, noting that the majority of defects have a size less than 2 nm.

Permoporosimetry technique is considered as a non-destructive and simple method for characterization of defects, especially those with a size less than 1 nm [23]. **Table 1** gives a summary of advantages and drawbacks of both direct and indirect characterization techniques.

Table 1

Advantages and drawbacks of characterization techniques of defects.

4. Sources of defects in zeolite membranes**4.1. Formation of defects during membrane preparation****4.1.1. Nature of the support**

The occurrence of defects could be originated from the support in terms of morphology and properties (roughness and thermal expansion). Generally, the degree of smoothness of the support should be optimized in a way to avoid the peeling off of the zeolite layer if the surface is very smooth or the absence of adherence between the layer and the support if the surface is very rough [57]. Zhou *et al.* attributed the formation of cracks in MFI zeolite membrane to the roughness ($R_a=907$ nm) of alumina support [58]. The support has a non-plate shape containing hills and pits as shown in **Fig. 10a-b**. The zeolite film takes the shape of the support during the crystallization of zeolite layer causing the formation of cracks in rough areas. Moreover, the authors affirmed the interest of polishing the support prior the deposition of zeolite layer. The adopted approach is highly likely lead to the acquisition of a defect-free membrane. However, in another study, it was shown that the smooth surface of the support might also develop cracks [59]. Two α -alumina supports with different morphologies and degrees of smoothness were used to prepare ZSM-5 and SSZ-13 membranes. One support has a very smooth surface, while the other is rougher and contains curvatures. It was found that more cracks are observed in the membrane prepared on the smooth support in comparison with the rougher support. The authors explained that the roughness makes the zeolite layer less attached to the support.

Zeolite membranes are grown on various supports geometry, like flat, tubular and monolithic configurations [60]. The preparation of zeolite membrane on monolithic support is more challenging since the control of the uniformity of seeds deposition on the support is difficult due to its geometry [61]. Ma *et al.* reported that silicate-1 zeolite membrane deposited on 61-

channel monolithic support exhibits some boundary defects [62]. This was attributed to the seeding step, in which the support was seeded using dip-coating method. The reproducibility of seeding on monolithic support should be improved. The types of defects able to occur during the seeding step are discussed in Section 4.1.3.

Coefficient of thermal expansion (CTE) of the support also plays a crucial role in controlling defects. A big difference in coefficients between the support and the zeolite produces thermal stress that could induce cracks and grain boundaries [42]. It is of a vital importance to choose a support that has CTE comparable to the zeolite material. *Akhtar et al.* selected two supports with different CTEs to evidence their roles in defect formation in MFI zeolite membrane [42]. The first support was made of alumina (a commercial substrate), while the second support was prepared from silicate-1, which is made from the same material as the zeolite membrane. Alumina and silicate-1 have CTEs of $+ (8-8.8) \times 10^{-6}$ and $- (1-3) \times 10^{-6} \text{ } ^\circ \text{C}^{-1}$, respectively. The membrane supported by the alumina substrate contains cracks and grain boundaries because of the mismatch between the zeolite layer and the support, which resulted from the difference in CTEs. On the other hand, the membrane supported by the silicate-1 substrate is free from cracks due to the similarity of the CTEs of both the support and the zeolite layer. *Das et al.* evaluated the impact of the modification of clay- Al_2O_3 support with SiO_2 particles on the occurrence of defects in SAPO-34 membrane [63]. When the zeolite layer was deposited on an unmodified support, it was observed that zeolite crystals have random orientation at the surface of the membrane as displayed in **Fig. 11b**. Besides, a gap forms between the zeolite layer and the support. In the same context, *Deng et al.* reported that MFI zeolite membrane prepared on the unmodified α -alumina substrate developed grain boundaries, contrary to the membrane prepared on the modified support with the deposition of silica layer [64]. Silica provides silanol groups Si-OH at the surface of the support. The presence of hydroxyl groups promotes the nucleation and adherence of MFI zeolite crystals due to van der Waals interactions and H-

bonding between OH groups of the SAPO-34 crystals and OH groups of the modified silica support. For this reason, the modification of the substrate surface is highly recommended in order to enhance the nucleation and growth of the zeolite film [12,63].

Another parameter to consider is the curvature of the support that has an impact on defects occurrence. Zeolite membranes grown on a support with a curved surface, like tubular or hollow fiber supports, may face greater challenges related to thermal expansion phenomenon [65]. *Chen et al.* investigated the effect of surface curvature of Al₂O₃ hollow fiber support on defect formation in prepared MFI zeolite membrane [65]. It was found that supports with high curvatures exhibit more intercrystalline gaps in the membrane. This may result from the difference in thermal expansion coefficients of Al₂O₃ support and the MFI zeolite layer.

Fig. 10. SEM images of (a) hill and (b) pit at the surface of alumina support, (c) cracks at the foot of a hill and (d) at the bottom of a pit [58].

Fig. 11. Cross-view images of SAPO-34 membrane prepared on (a) modified (b) unmodified support [63].

4.1.2. Source of precursors

The crystallization of zeolite materials could be impacted by the source of Al and Si precursors because they control the zeolite phase. *Zhu et al.* selected 3 types of silica sources, namely colloidal silica (CS), precipitated silica (PS) and tetra-ethylorthosilicate (TEOS) to investigate which type is likely to generate defects in ZSM-5 zeolite membrane [66]. It was found that TEOS allows to obtain a discontinuous zeolite film and intercrystalline boundaries. This is attributed to the type of TEOS that is considered a monosilica, which is likely to form small zeolite crystals. On the other hand, the membrane prepared from PS shows amorphous materials that are resulted from the heterogenous gel containing precipitates of silica after crystallization. The study revealed that CS is the most appropriate to prepare a dense and continuous ZSM-5 layer. *Lee et al.* used sodium metasilicate and fumed silica for the preparation of NaA zeolite membrane [67]. The use of fumed silica as a Si source results in non-uniform coverage of the

support in addition to the presence of non-zeolitic pores and defects like pinholes as shown in **Fig. 12b**. This is related to the occurrence of sodalite phase coexisting with NaA zeolite. Contrarily, zeolite crystals using sodium metasilicate are dense and display a well-defined shape as shown in **Fig. 12a**. *Zhang et al.* tested various Al sources for the synthesis of NaA zeolite including aluminum sulfate, aluminum isopropoxide, aluminum hydroxide and alumina [68]. The experimental results show that the Al precursor highly impacts the zeolite crystal phase. Aluminum sulfate and aluminum isopropoxide allow to obtain NaA zeolite crystals, while aluminum hydroxide leads to sodalite phase with traces of NaA zeolite crystals. However, alumina results in the formation of amorphous phase.

Fig. 12. SEM images of synthesized NaA zeolite membranes from (a) sodium metasilicate (defect-free membrane) (b) fumed silica (defective membrane) [67].

4.1.3. Seeding technique

Seeding step plays a major role in preparing defect-free membrane. Existing seeding techniques reported in the literature include dip-coating, spin-coating, rub-coating, dry rolling, vacuum seeding, etc. [69–72]. The efficiency of seeding methods could be linked to the shape and the roughness of the support and could also be related to the number of seeding cycles. *Isa et al.* examined the impact of dip-coating and vacuum seeding on the preparation of uniform NaY zeolite membrane [45]. It was observed that the seeded membrane using vacuum seeding exhibits cracks due to the effect of vacuum. This latter force leads to the accumulation of seeds on the surface of the support, resulting in the formation of a thick layer. The increase in the thickness may increase the probability of developing cracks during hydrothermal treatment. Dip-coating method leads to the apparition of pinhole-like defects on the upper surface of the zeolite membrane due to the incomplete seeding of the support. During dip-coating, capillary and gravitation forces are responsible of the transport of seeds towards the support. When the

support is saturated with water by capillary force, the transport of seeds is stopped. This is the reason for the incomplete coverage of the support.

Alam et al. reported the problems associated with manual seeding during the preparation of SAPO-34 zeolite membrane, and compared the results to other seeding technique *i.e.*, dry rolling [69]. When the membrane undergoes manual seeding, the resulting layer is heterogeneous with low coverage of zeolite seeds, which indicates that the layer is defective. The zeolite layer formed by the dry rolling technique is homogeneous and compact. However, it should be noted that the parameters controlling the dry rolling technique may also cause defects such as broken seeds on the support surface due to mechanical forces caused by high rolling speed. **Table 2** provides a summary of some seeding techniques that have been detailed in the literature and their corresponding defects.

The variation of particle size of seed may also result in defects formation. *Nazir et al.* investigated the effect of three seed sizes ranging from 750 to 5500 nm on the formation of NaX zeolite layer [73]. Membranes synthesized with the largest seeds exhibit more visible intercrystalline gaps. On the other hand, membranes prepared with smaller seed sizes displays better zeolite crystals intergrowth. This reveals that employing larger seeds promotes the occurrence of defects. These findings are consistent with the results reported by *Wang et al.* [74]. The authors studied nanosized (50 nm) and commercial micro-sized seed (0.7-1.4 μm) in the preparation of FAU zeolite membrane. The produced membrane using micron-sized seeds exhibits micron-scale voids within the membrane layer. Comparatively, the smaller gaps between nanoseeds leads to reduce defects in the FAU zeolite membrane.

Table 2

Seeding techniques of zeolite membranes.

4.1.4. Crystallization kinetics

Synthesis process of zeolite membranes is considered a complex operation because several parameters are involved at the same time. These parameters control the purity of synthesized zeolite material, structural properties, amount of defects and membrane thickness. This section focuses on the effect of temperature, time of crystallization, and Si/Al ratio on defect formation.

4.1.4.1. Crystallization time

It is known that crystallization time is the main factor that controls the thickness of the membrane. In general, short synthesis time allows the formation of thinner membranes that have a greater chance of developing defects in comparison to thicker membranes [24]. *Sakai et al.* assessed the impact of varying crystallization time from 6 to 336 h on the defect formation in silicate-1 zeolite membrane [77]. When the crystallization time comprises between 72 and 120 h, the membrane exhibits a significant amount of grain boundaries defects resulting from the incomplete crystals growth. As the crystallization time increases, the membrane becomes thicker and presents only a few defects. In the same context, *Wang et al.* demonstrated that short synthesis time causes incomplete growth of MFI zeolite layer [78]. However, they have found that a short synthesis time could be sufficient if it is accompanied by multiple hydrothermal cycles. They observed that there is less attachment between zeolite crystals after one hydrothermal cycle. Whilst, when the number of cycles increases from 1 to 2 cycles of 2 h of crystallization, the defects are remarkably reduced.

The synthesis time may induce a phase transformation of the zeolite, which is also considered a form of defect. For instance, when the time of synthesis prolongs during the preparation of NaA zeolite membrane, then NaA zeolite undergoes phase transformation to SOD zeolite. This transition creates intercrystalline pores, which would be responsible for cracks formation [18]. *Mu et al.* studied the effect of synthesis time on the creation of defects in SAPO-34 zeolite membrane by modifying the time from 8 to 22 h during the synthesis stage [14]. For a synthesis time of 8 h, the prepared membrane is thinner compared with the membrane produced after 22

h. This long time of synthesis causes the formation of intercrystalline defects that are probably due to insufficient time of crystal growth.

4.1.4.2. Crystallization temperature

Synthesis temperature is also considered a crucial parameter that may cause the creation of defects in zeolite membranes. Synthesis temperature mostly generates the transformation of zeolite phase and/or formation of other zeolite impurities [79]. *Achiou et al.* demonstrated that increasing the temperature of synthesis from 60 to 80 °C during the synthesis of NaA zeolite membrane promotes the crystallization of P-type zeolite which is an undesired zeolite phase (Fig.13) [19]. Moreover, this increase in temperature results in a reduction in the size of zeolite crystals. Elsewhere [80], zeolite Y also displays a change of phase with the variation of synthesis temperature from 85 to 100 °C. It was observed that an amorphous phase is formed beside zeolite Y at 85 °C, and this is attributed probably to the small size of zeolite Y particles. While at 90 °C, a pure zeolite Y was synthesized. Once the temperature was raised to over 90 °C, it was found that another zeolite phase appears, which is zeolite P. The change in temperature has a strong impact on the crystallization kinetics of zeolites, including nucleation and crystal growth. The increase in temperature favors the growth of crystals, whereas the decrease of temperature promotes nucleation, resulting in small zeolite crystals [80]. *Jafari et al.* varied the crystallization temperature from 80 to 100 °C during the preparation of A-type zeolite membrane [81]. When the temperature was between 80 and 100 °C, the formed zeolite layer is not uniform and some pinholes are detected on the surface of the membrane due to the incomplete growth of the zeolite layer. It was found that 100 °C is the appropriate temperature to obtain a membrane with high crystallinity. *Liu et al.* studied the impact of crystallization temperature in the range of 100-120 °C on the preparation of Si-rich LTA zeolite membrane [82]. It was reported that the increase in the temperature leads to an improvement in crystallinity in the studied temperature interval. However, when the temperature exceeds 120 °C, inter-

crystalline boundaries take place in Si-rich LTA membrane. These defects could occur because of the presence of impurity crystals that form at high temperatures. Furthermore, zeolite crystals go from a smooth edge to a sharp cubic crystal when the crystallization temperature is increased, which implies that the crystallinity of zeolite is also impacted.

Fig.13. SEM images of synthesized membranes at (a) 60 °C and (b) 80 °C [19].

4.1.4.3. Si/Al ratio

The composition of the batch synthesis has a significant role in ensuring the absence of defects in the zeolite membrane. Basically, when the Si/Al ratio in the batch synthesis is high, the membrane exhibits fewer defects than a membrane with a low Si/Al in the batch [24]. *Yu et al.* studied the influence of the Si/Al ratio on the creation of defects in NaA zeolite membrane [17]. Si/Al ratio was varied from 5 to 9 in the synthesis batch. Cracks occur at the surface and the bottom of the zeolite layer at Si/Al ratio of 5 and 6. Additionally, holes are also detected in the single crystal surface for Si/Al ratio of 6. When the Si/Al ratio is increased to 9, the obtained layer is discontinuous, and the crystals exhibit a spherical morphology that is different from that of NaA zeolite. In another work, the Si/Al ratio in batch synthesis of CHA zeolite membrane was augmented from 20 to 100. It was revealed that as the Si/Al ratio increases, the defects density decreases [83]. At a low Si/Al ratio of 20, CHA zeolite membrane presents cracks between the zeolite layer and substrate, and then they propagate to the interface. However, when the Si/Al ratio increases the amount of cracks decreases and are smaller than those present in CHA membrane with Si/Al ratio of 20. *Kosinov et al.* investigated the effect of variation of Si/Al ratio from 5 to 100 in the batch synthesis on the appearance of defects in SSZ-13 zeolite membrane [13]. The membrane exhibits grain boundaries when batch synthesis contains a Si/Al ratio of 5. However, when the Si/Al ratio is increased to 100 zeolite crystals are well grown. The behavior of defects with the variation in Si/Al ratio is shown in **Fig.14**. It

reveals that when the Si/Al ratio increases, the number of grain boundaries is significantly diminished.

The increase/decrease in Si/Al ratio could also be responsible of the occurrence of defects in the form of impurity phases. *Wang et al.* demonstrated that the increase in the Si/Al ratio from 10 to 40 for the preparation of FAU membrane results in the formation of NaP zeolite crystals [74]. This impurity phase in the membrane layer could easily lead to the formation of inter-crystalline defects, pinholes and cracks. *Conato et al.* confirmed that the change in the Si/Al ratio impacts the formation of zeolite phase [84]. For example, the increase or decrease in the Si/Al ratio for the formation of FAU zeolite could lead to the appearance of binary phases notably FAU and GIS (polymorphs zeolite P).

Fig. 14. Hydrogen flux through defects SSZ-13 zeolite membrane [13].

4.1.5. Membrane thickness

It is well-known that there is a strong relationship between the thickness of the zeolite layer and the amount of defects. Generally, with the decrease in membrane thickness, the membrane has a greater chance to form defects. On the other hand, it is obvious that the selectivity of the membrane could increase with the increase of membrane thickness, but in the presence of defects, the selectivity is strongly impacted. *Qiu et al.* evaluated the presence of defects in thin and thick SSZ-13 zeolite membrane by comparing their performances in the separation of CO₂/CH₄ [85]. It was found that the thin membrane is more defective than the thick membrane. The authors explained that defects are more likely to take place in thin membranes because there are grain boundaries that could be resulted from the gaps between crystals that have small sizes. It is generally assumed that the amount of cracks could increase when the membrane thickness decreases [86]. However, *Sakai et al.* demonstrated that thick membranes could also develop cracks [77]. For instance, silicate-1 zeolite membrane exhibits more cracks when the

thickness increases [77]. It is important to optimize membrane thickness in order to achieve high membrane selectivity.

4.1.6. Template removal

The selection of the template is crucial because it affects the physicochemical properties of synthesized zeolite, phase purity and crystal size [24]. It is necessary to eliminate the template to maintain the microstructure of zeolite. This step is considered crucial during membrane preparation because it could be responsible for the creation of defects in zeolite membranes, especially cracks [87].

The most common method of template removal is calcination [88,89], which is usually carried out at high temperatures (superior to 400 °C) with a slow heating rate to not generate defects. However, calcination is always accompanied with thermal stress [90], which refers to shrinkage of the zeolite layer [91]. Increasing the calcination temperature could increase defects generation [92]. *Nai et al.* evaluated the size and distribution of defects after template removal via calcination at 450 and 550 °C during the preparation of Fe-ZSM-5 membrane. The calcined membrane at 550 °C presented much higher amount and larger defects than the membrane calcined at 450 °C. At 450 °C, the percentage of defects was estimated to be 31.1% of the total open area, including mesoporous and microporous defects (0.6-2 and 2-6 nm, respectively), while at 550 °C, the percentage of defects could reach 78%.

Donato and coworkers compared the effect of two heating profiles on the formation of defects in MFI zeolite membrane during template (tetrapropylammonium) removal [93]. The first heating profile is fast, reaching 450 °C in 8 h, while the slow profile reaches 450 °C after 24 h. Afterwards, the membrane is maintained at 450 °C for 2 h, which means that in total, the operating time was reduced by 14 h from the slow to the fast profile. Fast thermal treatment induces more cracks in the zeolite layer than slow treatment. The authors found that this could be created because template removal encourages the accumulation of gaseous species inside

the layer, causing cracks. On the other hand, the expansion phenomenon could also explain the cracks appearance considering the dissimilarity of the expansion coefficients of MFI zeolites and alumina support.

To avoid or reduce defects generated during the calcination, it is recommended to adopt new approaches such as ozonation [94] and rapid thermal processing (RTP) [95]. *Lee et al.* demonstrated the interest and efficiency of using RTP prior the conventional calcination during the template removal in SAPO-34 zeolite membrane [48]. During RTP, the membrane was heated to 700 °C within 1 min, then it was cooled using water recirculation. Afterwards, the membrane was subjected to conventional calcination at 480 °C for 10 h at a rate of 0.5 °C/min. It was found that the selectivity of the membrane is improved, which means that grain boundaries are reduced. In another work, different approaches of template removal were used to compare their contribution to defects formation in SAPO-34 zeolite membrane [96]. The first approach is conventional calcination at 400 °C for 4 h. The second one is RTP at 700 °C for 1 min, then cooling to 400 °C followed by conventional calcination at the same temperature for 4 h. It was found that RTP favors the decomposition of the template which participates in cracks reduction. This finding is also confirmed by the increase of selectivity by 80% of the membrane treated by RTP compared to the conventional calcined membrane.

Ozonation technique is also used to remove the template from the zeolite layer with oxidation in an ozone environment at low temperatures. *Wang and coworkers* utilized this method for the removal of template from DDR zeolite membrane at 200 °C in the O₃/O₂ mixture [97]. It was found that cracks don't occur contrarily to calcined membrane. The sufficient time to remove totally the template was estimated to over 60 h. From this, it is seen that this method requires a long time to the complete removal of the template. The advantages and drawbacks of the cited template removal methods are presented in Table 3.

Table 3.

Advantages and inconvenient of the cited template removal methods.

4.2. Formation of defects related to membrane application

It is well known that the framework structure of zeolite membranes could be affected during application, leading to the generating of defects. It was reported that the structure of MFI zeolite membrane could change when separating organics/water mixture [16]. Water content and the operating temperature were found to have a considerable impact on the stability of MFI zeolite membrane. At 80 °C, the crystallinity and structure of MFI zeolite membrane are damaged. As a result, silanol defects are formed because of hydrolysis of the MFI zeolite membrane. When separating ABE (acetone, butanol and ethanol) aqueous solution via the pervaporation process, it was observed that there is amorphous silica in the zeolite membrane, and the shape of edges and corners become indistinguishable after pervaporation. This phenomenon refers to the corrosion of zeolite crystals [16]. Elsewhere [98], it was demonstrated that MFI zeolite layer remains instable after pervaporation experiments for separation of ethanol/water mixtures varying the temperature from 60 to 140 °C. Internal defects that take the form of silanol groups are formed in the membrane because of the presence of hydroxide ions in alkaline media. The MFI zeolite membrane remains unstable because of the reaction between ethanol and silanol groups. As a result, MFI zeolite crystals significantly dissolve after 6 h of pervaporation due to the hydrolysis phenomenon that takes place when the zeolite membrane is exposed to water at high temperatures (110 and 140 °C). However, at lower operating temperatures, the MFI zeolite membrane is more stable during the separation of butanol/water mixture. LTA zeolite membrane is affected during water immersion depending on exposure time [99]. When the membrane is in contact with water for 3 days, the zeolite layer degrades as shown in **Fig. 15**, caused by the dissolution of LTA zeolite layer. It was supposed that this defect does not propagate to the interface between the support and the zeolite layer. After 12 days of contact,

the dissolution is stronger and propagates in the surface, beside the appearance of interconnected cracks due to dealumination/desilication process.

Qu et al. studied the effect of water adsorption onto NaA zeolite membrane behavior during the dehydration of alcohols (ethanol, methanol and isopropanol) [54]. They concluded that NaA zeolite undergoes expansion as the water feed increases, which results in reduction of defects. It can be evidenced from all these studies that water content in the feed strongly affects the stability of zeolite membranes.

The application of zeolite membranes in acid media is responsible for defect creation and acid-corrosion during pervaporation experiments [100]. Acids could damage the zeolite membrane framework due to the dissolution process, and cracks formation could take place [101]. CHA zeolite membrane shows cracks after dehydration of acetic acid. On the other hand, dealumination phenomenon in the zeolite framework also takes part. This means that the Si/Al ratio of the zeolite is changed. More specifically, this ratio is increased after pervaporation experiments. Grain boundaries could also appear in acidic media for Al-rich zeolite framework, like MOR, because of the dealumination process that manifests easily [102]. *Hasegawa et al.* studied the stability of NaA zeolite membrane in acid medium, varying the contact time from 5 to 100 min [103]. NaA zeolite membrane shows cracks in contact with sulfuric acid for 50 and 100 min as displayed in **Fig. 16b-c**, and an amorphous-like material is seen on the surface of the membrane treated with acid for 50 min. Furthermore, hydrolysis leads to the dissociation of Si-O and/or Al-O bonds, which causes destruction of the structure. The Si/Al ratio also decreases from 1.06 to 0.51 after 100 min of exposure to acid. Moreover, the membrane becomes thinner with the increase in contact time.

In another study, exposure to methanol during the separation of CH₃OH/H₂ mixture leads to the destruction of the structure of SOD zeolite membrane [104]. When SOD crystals are exposed to 5% methanol at 240 °C for 3 h, the structure is deformed. Increasing the feed temperature to

270 °C caused the complete agglomeration and dissolution of SOD crystals, which reveals that the sodalite structure is not stable under these operating conditions.

Fig.15. Top-view SEM images of LTA zeolite membrane after (a) 3 days and (b) 12 days of water exposure [99]

Fig. 16. SEM images of NaA zeolite membrane after (a) 5 min, (b) 50 min and (c) 100 min of treatment by solutions containing 0.1 mL of sulfuric acid [103].

5. Reparation techniques of defects in zeolite membranes

In order to achieve high separation performance, the zeolite membrane has to be free from any kind of defect. This perfect membrane is rarely achievable, especially for the fabrication of membranes with large surfaces. Therefore, it is necessary to adopt a reparation approach to eliminate defects in zeolite membranes when it is tricky to avoid defects formation [23]. Researchers have worked on the development of diverse methods to successfully treat defects. Various strategies were studied, and they could be classified into two approaches. The first approach is related to the optimization of synthesis method during the preparation of the membrane, while the second approach concerns the repair of defects after membrane preparation and is referred to as post-treatment methods [86]. In some cases, the modification of the synthesis process might be efficient for defect reparation. For instance, it is well known that microwave heating is recognized as a good method to prepare zeolite membranes with no or few defects [105]. *Wei et al.* proposed a novel method to patch defects in NaA zeolite membrane during preparation. In this method, the synthesis solution is supplemented with methylcellulose (MC) in order to control the growth of zeolite crystals. Additionally, MC can be easily removed after membrane preparation [105]. The mechanism of synthesis is explained as follows: Si/Al content in the hydrogel penetrate the pores of the support, while MC particles are hardly adsorbed because of their molecular mass. Consequently, a protective layer is formed during microwave heating due to the gelification of adsorbed MC particles. Thus, it helps to

avoid the accumulation of Si and Al content on the surface of the support. Furthermore, it was also proved that the number and size of defects decrease with the increase of the synthesis cycles (multi-stage synthesis).

Post-treatment method consists in blocking defects after membrane preparation using molecule that has a specific size to enter in defects, but does not access to zeolite pores. **Fig. 17** displays two possibilities for healing defects after membrane preparation.

Vaccum-wiping deposition (VWD) method was tested to repair defects in beta zeolite membrane using spherical polyelectrolyte complex (PEC) nanoparticles [44]. PEC nanoparticles were used as a filler to penetrate into cracks generated during calcination. PEC nanoparticles have the advantage of stable ionic cross-linking, which means that PEC nanoparticles have strong polarity that enhances the diffusion in the membrane [44]. After the reparation of defects, the membrane was tested for the separation of methanol/methyl tert-butyl ether mixture, which shows that the flux decreases with the increase of VWD cycles. More importantly, it was proven that this repair method significantly improves the selectivity of the membrane.

Vacuum assisted deposition (VAD) was reported by *Mu et al.* to patch intercrystal/cracks defects in SAPO-34 zeolite membrane using porous organosilica as shown in **Fig. 18** [14]. Three VAD cycles were considered optimal to cover only the cracks rather than covering zeolite crystals with organosilica, which was selected thanks to its nanopore structure. The membrane was tested for CO₂/CH₄ separation after reparation and shows that the selectivity is remarkably enhanced by a factor of 2-3 compared to the untreated membrane. *Xu et al.* used also the same technique using sodium alginate to eliminate non-zeolitic pores in NaA zeolite membrane [106]. Sodium alginate molecule was selected as a filler due to its capacity to form an ionic-cross-linking hydrogel. After VAD treatment, the separation factor of the membrane is enhanced seven times.

Korelskiy et al. used coking technique to block grain boundaries of MFI zeolite membrane using isopropanol as a coke precursor [107]. Coke formation was carried out at 350 °C and varying the time from 1 to 25 h. This treatment leads to a 70% decrease in permeance through defects when increasing the coking time to 25 h, which means that grain boundaries are blocked.

In another work, micro-defects repairation was studied in ZSM-5 zeolite membrane using CVD technique [86]. It was demonstrated that this method is efficient for reducing defects that have a size smaller than 2 nm via the deposition of carbon in the defects. It should be noted that it is recommended to work at temperatures below 800 °C to avoid cracks creation during CVD for ZSM-5 zeolite membrane. The membrane selectivity for H₂/SF₆ and He/SF₆ increases after treatment, which confirms the success of the CVD technique in sealing micro-defects.

Karimi and co-workers give a simple method to plug grain boundaries in MFI zeolite membrane through the deposition of amorphous silica layer on the surface of the membrane [56]. The membrane was dipped in a polymeric silica solution and then calcined. Permprometry data reveal the reduction of the amount of grain boundaries from 0.19 to 0.12% from the total membrane area after modification. The separation factor of CO₂/H₂ increases from 8.5 to 36.0 after modification, while the CO₂ flux declines by 40%.

Zhou et al. studied the healing of defects on SSZ-13 zeolite membrane using chemical liquid deposition technique [108]. Experimentally, two steps are taken place: (i) silanization by siloxane polymer on the surface of the membrane, and (ii) polymerization of the siloxane in order to form a polymer layer on the top of the membrane. The advantage of this method is energy saving since it operates at lower temperatures, like 80 °C, compared to CVD, which operates at 800 °C. After membrane repairation, the selectivity of CO₂/CH₄ increases by a factor of 9 while the CO₂ permeance decreases by 15%.

Molecular layer deposition (MLD) technique was used to reduce non-selective defects/inter-crystalline pores in SSZ-13 zeolite membrane [109]. MLD consists in creating organic-

inorganic thin coatings on the membrane substrate in order to control non-zeolitic pore size. *Dong et al.* used TiCl_4 and ethylene glycol as precursors for the MLD modification. The study showed that MLD may block the defects in the membrane.

Therefore, it can be concluded that reparation techniques are important to improve zeolite membranes performances and are required when it is very hard to avoid defects formation. Generally, post-treatment methods of zeolite membranes could help to achieve higher selectivity accompanied with loss in permeability. However, it is worth noting that these methods may present some drawbacks. For instance, they could damage the zeolite membrane in the case of high temperatures during treatment [44]. Also, the reparation methods are costly since they require high operating temperatures. **Table 4** summarizes of some strategies used to repair or reduce defects.

Table 4

Methods of reparation of defects in zeolite membranes.

Fig. 17. Methods of healing defects in zeolite membranes [25].

Fig. 18. Defects healing in SAPO-34 zeolite membrane using VAD technique [14].

6. Conclusion and perspectives

Zeolite membranes possess significant potential for use in liquid and gas separations owing to their unique properties that make them unique materials for separation technology. Despite considerable efforts, several limitations persist in scaling zeolite membranes. The primary challenge lies in preparing defect-free zeolite membranes. Defects affect membrane selectivity by allowing molecules to permeate through non-selective pathways. The preparation of thin, defect-free membranes with high flux without compromising selectivity is highly demand. Thus, developing efficient strategies to eliminate or minimize defects is crucial.

This review comprehensively explores the complex phenomenon of defects in zeolite membranes with the aim of elucidating their origins. It provides a detailed guideline for both industrial and scientific researchers is zeolite membrane, with key points outlined as follows:

- Defects typically occur during membrane preparation or within applications. They may also arise due to the instability of zeolite membranes in certain solvents or acidic media under specific conditions.

- Achieving defect-free zeolite membranes can be accomplished by precisely controlling synthesis parameters to optimize nucleation and growth steps. Crucial parameters include time and temperature of crystallization, concentration and nature of precursors, seeding techniques, and the nature and properties of the membrane support.

- Various techniques for characterizing defects in zeolite membranes can be employed to elucidate morphology and quantify defects. The advantages and drawbacks of each technique are presented to aid in selecting appropriate characterization techniques for targeted defects.

- Significant advances have been made in repairing defects in zeolite membranes, particularly when their creation is difficult to avoid. These methods help enhance membrane selectivity. Healing methods are categorized into two approaches: optimizing membrane preparation and using post-treatment methods after membrane preparation. Post-treatment methods efficiently reduce defects in zeolite membranes; however, some methods may lead to additional issues like pore blockage, especially those based on filling defects such as coke deposition. A summary of post-treatment methods is provided to determine the appropriate technique for each type of defect. Despite significant research progress in zeolite membrane preparation, existing studies do not provide a complete understanding of defect control.

The authors propose that future research on zeolite membranes should focus more on the aspect of defects. Directions from this review include:

- Identifying and classifying different types of defects in zeolite membranes, with an advanced classification considering morphology, size and source of the defect.
- Deepening understanding of the formation mechanisms of defects in zeolite membranes through fundamental analyses of mechanisms like nucleation and growth of zeolites, which can improve various approaches to membrane preparation and enhance reproducibility.
- Employing advanced characterization techniques to reveal all types of defects, especially microdefects, for evidencing morphology and size.

Declaration of competing interest

The authors declare that they do not have any personal relationships or financial problems that could influence the work.

CRediT Authors contribution

F.Z. Charik: Writing-original draft, **B. Achiou:** Review and Editing, **A. Belgada:** Writing-original draft, **M. Ouammou:** Validation, **M. Rabiller-Baudry:** Supervision, **S. Alami Younssi:** Supervision.

Acknowledgments

This work was supported by MESRSFC (Ministère de l'Enseignement Supérieur et de la Recherche Scientifique et de la formation des cadres-Morocco) and CNRST (Centre National pour la Recherche Scientifique et Technique-Morocco) (Project : PPR/2015/72).

Fatima Zohra Charik acknowledges Eiffel & Campus France for the PhD grant n°EIFFEL-DOCTORAT 2020/n°P757215H.

References

- [1]C. Algieri, E. Drioli, Zeolite membranes: Synthesis and applications, Sep. Purif. Technol. 278 (2021) 119295. <https://doi.org/10.1016/j.seppur.2021.119295>.
- [2]F.Z Charik, B.Achiou, A.Belgada, M.Ouammou, S.A Younssi, Zeolite materials in service of membrane technology, in: Zeolites Adv. Reserach Appl., Nova Science Publishers, 2020: pp. 133–162.

- [3] M.S. Nabavi, T. Mohammadi, M. Kazemimoghadam, Hydrothermal synthesis of hydroxy sodalite zeolite membrane: Separation of H₂/CH₄, *Ceram. Int.* 40 (2014) 5889–5896. <https://doi.org/10.1016/j.ceramint.2013.11.033>.
- [4] X. Lu, H. Wang, Y. Yang, Z. Wang, Microstructural manipulation of MFI-type zeolite films/membranes: Current status and perspectives, *J. Membr. Sci.* 662 (2022) 120931. <https://doi.org/10.1016/j.memsci.2022.120931>.
- [5] S. Boycheva, D. Zgureva, H. Lazarova, M. Popova, Comparative studies of carbon capture onto coal fly ash zeolites Na-X and Na-Ca-X, *Chemosphere* 271 (2021) 129505. <https://doi.org/10.1016/j.chemosphere.2020.129505>.
- [6] A.A. Ahmed, Z.H. Yamani, Synthesis and characterization of SnO₂-modified ZSM-5 zeolite for hydrogen gas sensing, *Mater. Chem. Phys.* 259 (2021) 124181. <https://doi.org/10.1016/j.matchemphys.2020.124181>.
- [7] N. Kosinov, J. Gascon, F. Kapteijn, E.J.M. Hensen, Recent developments in zeolite membranes for gas separation, *J. Membr. Sci.* 499 (2016) 65–79. <https://doi.org/10.1016/j.memsci.2015.10.049>.
- [8] A. Belgada, B. Achiou, S. Alami Younssi, F.Z. Charik, M. Ouammou, J.A. Cody, R. Benhida, K. Khaless, Low-cost ceramic microfiltration membrane made from natural phosphate for pretreatment of raw seawater for desalination, *J. Eur. Ceram. Soc.* (2020) S0955221920307913. <https://doi.org/10.1016/j.jeurceramsoc.2020.09.064>.
- [9] A. Belgada, F.Z. Charik, B. Achiou, T. Ntambwe Kambuyi, S. Alami Younssi, R. Beniazza, A. Dani, R. Benhida, M. Ouammou, Optimization of phosphate/kaolinite microfiltration membrane using Box–Behnken design for treatment of industrial wastewater, *J. Environ. Chem. Eng.* 9 (2021) 104972. <https://doi.org/10.1016/j.jece.2020.104972>.
- [10] F.Z. Charik, B. Achiou, A. Belgada, Z.C. Elidrissi, M. Ouammou, M. Rabiller-Baudry, S.A. Younssi, Optimal preparation of low-cost and high-permeation NaA zeolite membrane for effective ethanol dehydration, *Microporous Mesoporous Mater.* 344 (2022) 112229. <https://doi.org/10.1016/j.micromeso.2022.112229>.
- [11] C.H. Cho, K.Y. Oh, S.K. Kim, J.G. Yeo, P. Sharma, Pervaporative seawater desalination using NaA zeolite membrane: Mechanisms of high water flux and high salt rejection, *J. Membr. Sci.* 371 (2011) 226–238. <https://doi.org/10.1016/j.memsci.2011.01.049>.
- [12] J. Zhou, C. Zhou, K. Xu, J. Caro, A. Huang, Seeding-free synthesis of large tubular zeolite FAU membranes for dewatering of dimethyl carbonate by pervaporation, *Microporous Mesoporous Mater.* 292 (2020) 109713. <https://doi.org/10.1016/j.micromeso.2019.109713>.
- [13] N. Kosinov, C. Auffret, G.J. Borghuis, V.G.P. Sripathi, E.J.M. Hensen, Influence of the Si/Al ratio on the separation properties of SSZ-13 zeolite membranes, *J. Membr. Sci.* 484 (2015) 140–145. <https://doi.org/10.1016/j.memsci.2015.02.044>.

- [14] Y. Mu, H. Chen, H. Xiang, L. Lan, Y. Shao, X. Fan, C. Hardacre, Defects-healing of SAPO-34 membrane by post-synthesis modification using organosilica for selective CO₂ separation, *J. Membr. Sci.* 575 (2019) 80–88. <https://doi.org/10.1016/j.memsci.2019.01.004>.
- [15] C. Chen, Y. Cheng, L. Peng, C. Zhang, Z. Wu, X. Gu, X. Wang, S. Murad, Fabrication and stability exploration of hollow fiber mordenite zeolite membranes for isopropanol/water mixture separation, *Microporous Mesoporous Mater.* 274 (2019) 347–355. <https://doi.org/10.1016/j.micromeso.2018.09.010>.
- [16] Z. Wu, L. Peng, C. Zhang, X. Wang, H. Liu, J. Wang, W. Yan, X. Gu, Extraction of butanol from ABE solution by MFI zeolite membranes, *Sep. Purif. Technol.* 242 (2020) 116771. <https://doi.org/10.1016/j.seppur.2020.116771>.
- [17] J. Yu, J. Zhang, C. Bao, Z. Zhang, H. Li, H. Xu, Controllable growth of defect-free zeolite protective layer on the surface of Pd membrane for chemical stability enhancement, *Microporous Mesoporous Mater.* 244 (2017) 119–126. <https://doi.org/10.1016/j.micromeso.2017.02.063>.
- [18] L. Wang, J. Yang, J. Wang, W. Raza, G. Liu, J. Lu, Y. Zhang, Microwave synthesis of NaA zeolite membranes on coarse macroporous α -Al₂O₃ tubes for desalination, *Microporous Mesoporous Mater.* 306 (2020) 110360. <https://doi.org/10.1016/j.micromeso.2020.110360>.
- [19] B. Achiou, D. Beqqour, H. Elomari, A. Bouazizi, M. Ouammou, M. Bouhria, A. Aaddane, K. Khiat, S. Alami Younsi, Preparation of inexpensive NaA zeolite membrane on pozzolan support at low temperature for dehydration of alcohol solutions, *J. Environ. Chem. Eng.* 6 (2018) 4429–4437. <https://doi.org/10.1016/j.jece.2018.06.049>.
- [20] A. Hasanzadeh, S. Pakdel, J. Azamat, H. Erfan-Niya, A. Khataee, Atomistic understanding of gas separation through nanoporous DDR-type zeolite membrane, *Chem. Phys.* 540 (2021) 110985. <https://doi.org/10.1016/j.chemphys.2020.110985>.
- [21] J. Hedlund, D. Korelskiy, L. Sandström, J. Lindmark, Permporometry analysis of zeolite membranes, *J. Membr. Sci.* 345 (2009) 276–287. <https://doi.org/10.1016/j.memsci.2009.09.012>.
- [22] S. Hong, D. Kim, H. Richter, J.-H. Moon, N. Choi, J. Nam, J. Choi, Quantitative elucidation of the elusive role of defects in polycrystalline MFI zeolite membranes on xylene separation performance, *J. Membr. Sci.* 569 (2019) 91–103. <https://doi.org/10.1016/j.memsci.2018.10.005>.
- [23] H. Maghsoudi, Defects of Zeolite Membranes: Characterization, Modification and Post-treatment Techniques, *Sep. Purif. Rev.* 45 (2016) 169–192. <https://doi.org/10.1080/15422119.2015.1103270>.
- [24] J. Xu, K.-G. Haw, Z. Li, S. Pati, Z. Wang, S. Kawi, A mini-review on recent developments in SAPO-34 zeolite membranes and membrane reactors, *React. Chem. Eng.* (2021) 10.1039/D0RE00349B. <https://doi.org/10.1039/D0RE00349B>.
- [25] I.C. Medeiros-Costa, E. Dib, N. Nesterenko, J.-P. Dath, J.-P. Gilson, S. Mintova, Silanol defect engineering and healing in zeolites: opportunities to fine-tune their properties and performances, *Chem. Soc. Rev.* 50 (2021) 11156–11179. <https://doi.org/10.1039/D1CS00395J>.

- [26] F. Dorosti, L. Ge, H. Wang, Z. Zhu, A path forward: Understanding and mitigating defects in polycrystalline membranes, *Prog. Mater. Sci.* 137 (2023) 101123. <https://doi.org/10.1016/j.pmatsci.2023.101123>.
- [27] P. Raizada, V. Soni, A. Kumar, P. Singh, A.A. Parwaz Khan, A.M. Asiri, V.K. Thakur, V.-H. Nguyen, Surface defect engineering of metal oxides photocatalyst for energy application and water treatment, *J. Materiomics* 7 (2021) 388–418. <https://doi.org/10.1016/j.jmat.2020.10.009>.
- [28] P. Rudolph, Fundamentals and engineering of defects, *Prog. Cryst. Growth Charact. Mater.* 62 (2016) 89–110. <https://doi.org/10.1016/j.pcrysgrow.2016.04.004>.
- [29] S. Bai, N. Zhang, C. Gao, Y. Xiong, Defect engineering in photocatalytic materials, *Nano Energy* 53 (2018) 296–336. <https://doi.org/10.1016/j.nanoen.2018.08.058>.
- [30] Z. Qin, W. Shen, S. Zhou, Y. Shen, C. Li, P. Zeng, B. Shen, Defect-assisted mesopore formation during Y zeolite dealumination: The types of defect matter, *Microporous Mesoporous Mater.* 303 (2020) 110248. <https://doi.org/10.1016/j.micromeso.2020.110248>.
- [31] M.E. Dose, K. Zhang, J.A. Thompson, J. Leisen, R.R. Chance, W.J. Koros, B.A. McCool, R.P. Lively, Effect of Crystal Size on Framework Defects and Water Uptake in Fluoride Mediated Silicalite-1, *Chem. Mater.* 26 (2014) 4368–4376. <https://doi.org/10.1021/cm500914b>.
- [32] M.S. Nabavi, M. Zhou, J. Mouzon, M. Grahn, J. Hedlund, Stability of colloidal ZSM-5 catalysts synthesized in fluoride and hydroxide media, *Microporous Mesoporous Mater.* 278 (2019) 167–174. <https://doi.org/10.1016/j.micromeso.2018.11.007>.
- [33] L. Sommer, D. Mores, S. Svelle, M. Stöcker, B.M. Weckhuysen, U. Olsbye, Mesopore formation in zeolite H-SSZ-13 by desilication with NaOH, *Microporous Mesoporous Mater.* 132 (2010) 384–394. <https://doi.org/10.1016/j.micromeso.2010.03.017>.
- [34] I. Grosskreuz, H. Gies, B. Marler, Alteration and curing of framework defects by heating different as-made silica zeolites of the MFI framework type, *Microporous Mesoporous Mater.* 291 (2020) 109683. <https://doi.org/10.1016/j.micromeso.2019.109683>.
- [35] X. Jia, W. Khan, Z. Wu, J. Choi, A.C.K. Yip, Modern synthesis strategies for hierarchical zeolites: Bottom-up versus top-down strategies, *Adv. Powder Technol.* 30 (2019) 467–484. <https://doi.org/10.1016/j.appt.2018.12.014>.
- [36] R. Zhang, R. Zou, W. Li, Y. Chang, X. Fan, On understanding the sequential post-synthetic microwave-assisted dealumination and alkaline treatment of Y zeolite, *Microporous Mesoporous Mater.* 333 (2022) 111736. <https://doi.org/10.1016/j.micromeso.2022.111736>.
- [37] D.V. Peron, V.L. Zholobenko, J.H.S. de Melo, M. Capron, N. Nuns, M.O. de Souza, L.A. Feris, N.R. Marcilio, V.V. Ordonsky, A.Y. Khodakov, External surface phenomena in dealumination and desilication of large single crystals of ZSM-5 zeolite synthesized from a sustainable source, *Microporous Mesoporous Mater.* 286 (2019) 57–64. <https://doi.org/10.1016/j.micromeso.2019.05.033>.

- [38] M.S. Holm, S. Svelle, F. Joensen, P. Beato, C.H. Christensen, S. Bordiga, M. Bjørgen, Assessing the acid properties of desilicated ZSM-5 by FTIR using CO and 2,4,6-trimethylpyridine (collidine) as molecular probes, *Appl. Catal. Gen.* 356 (2009) 23–30. <https://doi.org/10.1016/j.apcata.2008.11.033>.
- [39] D. Fodor, A. Beloqui Redondo, F. Krumeich, J.A. van Bokhoven, Role of Defects in Pore Formation in MFI Zeolites, *J. Phys. Chem. C* 119 (2015) 5447–5453. <https://doi.org/10.1021/jp5117933>.
- [40] X. Gao, Z. Wang, T. Chen, L. Hu, S. Yang, S. Kawi, State-of-art designs and synthesis of zeolite membranes for CO₂ capture, *Carbon Capture Sci. Technol.* 5 (2022) 100073. <https://doi.org/10.1016/j.ccst.2022.100073>.
- [41] J. Dong, Y.S. Lin, M.Z.-C. Hu, R.A. Peascoe, E.A. Payzant, Template-removal-associated microstructural development of porous-ceramic-supported MFI zeolite membranes, *Microporous Mesoporous Mater.* 34 (2000) 241–253. [https://doi.org/10.1016/S1387-1811\(99\)00175-4](https://doi.org/10.1016/S1387-1811(99)00175-4).
- [42] F. Akhtar, A. Ojuva, S.K. Wirawan, J. Hedlund, L. Bergström, Hierarchically porous binder-free silicalite-1 discs: a novel support for all-zeolite membranes, *J. Mater. Chem.* 21 (2011) 8822. <https://doi.org/10.1039/c1jm10584a>.
- [43] S. Park, M. Lee, S. Hong, Y. Jeong, D. Kim, N. Choi, J. Nam, H. Baik, J. Choi, Low-temperature ozone treatment for p-xylene perm-selective MFI type zeolite membranes: Unprecedented revelation of performance-negating cracks larger than 10 nm in polycrystalline membrane structures, *J. Membr. Sci.* 668 (2023) 121212. <https://doi.org/10.1016/j.memsci.2022.121212>.
- [44] Y. Li, B. Zhang, Defects repair and surface hydrophilic modification of zeolite beta membranes with spherical polyelectrolyte complex nanoparticles via vacuum-wiping deposition technique, *J. Membr. Sci.* 602 (2020) 117977. <https://doi.org/10.1016/j.memsci.2020.117977>.
- [45] M. Aimen Isa, T. Leng Chew, Y. Fong Yeong, Studies on Different Support Seeding Conditions Applied in the Formation of NaY Zeolite Membrane, *Mater. Today Proc.* 19 (2019) 1514–1523. <https://doi.org/10.1016/j.matpr.2019.11.176>.
- [46] J. Yu, J. Zhang, C. Bao, Z. Zhang, H. Li, H. Xu, Controllable growth of defect-free zeolite protective layer on the surface of Pd membrane for chemical stability enhancement, *Microporous Mesoporous Mater.* 244 (2017) 119–126. <https://doi.org/10.1016/j.micromeso.2017.02.063>.
- [47] H. Li, J. Wang, J. Xu, X. Meng, B. Xu, J. Yang, S. Li, J. Lu, Y. Zhang, X. He, D. Yin, Synthesis of zeolite NaA membranes with high performance and high reproducibility on coarse macroporous supports, *J. Membr. Sci.* 444 (2013) 513–522. <https://doi.org/10.1016/j.memsci.2013.04.030>.
- [48] T. Lee, J. Choi, M. Tsapatsis, On the performance of c-oriented MFI zeolite Membranes treated by rapid thermal processing, *J. Membr. Sci.* 436 (2013) 79–89. <https://doi.org/10.1016/j.memsci.2013.02.028>.

- [49] S. Hong, D. Kim, H. Richter, J.-H. Moon, N. Choi, J. Nam, J. Choi, Quantitative elucidation of the elusive role of defects in polycrystalline MFI zeolite membranes on xylene separation performance, *J. Membr. Sci.* 569 (2019) 91–103. <https://doi.org/10.1016/j.memsci.2018.10.005>.
- [50] G. Bonilla, Fluorescence confocal optical microscopy imaging of the grain boundary structure of zeolite MFI membranes made by secondary (seeded) growth, *J. Membr. Sci.* 182 (2001) 103–109. [https://doi.org/10.1016/S0376-7388\(00\)00549-4](https://doi.org/10.1016/S0376-7388(00)00549-4).
- [51] S. Al-Akwaa, D. Carter, F.H. Tezel, B. Kruczek, Characterization of defect-containing zeolite membranes by single gas permeation experiments before and after calcination, *J. Membr. Sci.* 629 (2021) 119269. <https://doi.org/10.1016/j.memsci.2021.119269>.
- [52] S.G. Sorenson, E.A. Payzant, W.T. Gibbons, B. Soydas, H. Kita, R.D. Noble, J.L. Falconer, Influence of zeolite crystal expansion/contraction on NaA zeolite membrane separations, *J. Membr. Sci.* 366 (2011) 413–420. <https://doi.org/10.1016/j.memsci.2010.10.043>.
- [53] S. Yang, Z. Cao, A. Arvanitis, X. Sun, Z. Xu, J. Dong, DDR-type zeolite membrane synthesis, modification and gas permeation studies, *J. Membr. Sci.* 505 (2016) 194–204. <https://doi.org/10.1016/j.memsci.2016.01.043>.
- [54] F. Qu, R. Shi, L. Peng, Y. Zhang, X. Gu, X. Wang, S. Murad, Understanding the effect of zeolite crystal expansion/contraction on separation performance of NaA zeolite membrane: A combined experimental and molecular simulation study, *J. Membr. Sci.* 539 (2017) 14–23. <https://doi.org/10.1016/j.memsci.2017.05.057>.
- [55] J.B. Lee, H.H. Funke, R.D. Noble, J.L. Falconer, High selectivities in defective MFI membranes, *J. Membr. Sci.* 321 (2008) 309–315. <https://doi.org/10.1016/j.memsci.2008.05.004>.
- [56] S. Karimi, D. Korelskiy, L. Yu, J. Mouzon, A. Ali Khodadadi, Y. Mortazavi, M. Esmaeili, J. Hedlund, A simple method for blocking defects in zeolite membranes, *J. Membr. Sci.* 489 (2015) 270–274. <https://doi.org/10.1016/j.memsci.2015.04.038>.
- [57] Y. Li, G. Zhu, Y. Wang, Y. Chai, C. Liu, Preparation, mechanism and applications of oriented MFI zeolite membranes: A review, *Microporous Mesoporous Mater.* 312 (2021) 110790. <https://doi.org/10.1016/j.micromeso.2020.110790>.
- [58] M. Zhou, M.S. Nabavi, J. Hedlund, Influence of support surface roughness on zeolite membrane quality, *Microporous Mesoporous Mater.* 308 (2020) 110546. <https://doi.org/10.1016/j.micromeso.2020.110546>.
- [59] N. Kosinov, C. Auffret, V.G.P. Sripathi, C. Gücüyener, J. Gascon, F. Kapteijn, E.J.M. Hensen, Influence of support morphology on the detemplation and permeation of ZSM-5 and SSZ-13 zeolite membranes, *Microporous Mesoporous Mater.* 197 (2014) 268–277. <https://doi.org/10.1016/j.micromeso.2014.06.022>.
- [60] Y. Lin, M.C. Duke, Recent progress in polycrystalline zeolite membrane research, *Curr. Opin. Chem. Eng.* 2 (2013) 209–216. <https://doi.org/10.1016/j.coche.2013.03.002>.

- [61] J. Zhou, S. Wu, B. Liu, R. Zhou, W. Xing, Scalable fabrication of highly selective SSZ-13 membranes on 19-channel monolithic supports for efficient CO₂ capture, *Sep. Purif. Technol.* 293 (2022) 121122. <https://doi.org/10.1016/j.seppur.2022.121122>.
- [62] B. Ma, Y. Zhu, H. Hong, L. Cui, H. Gao, D. Zhao, B. Wang, R. Zhou, W. Xing, Improved silicalite-1 membranes on 61-channel monolithic supports for n-butane/i-butane separation, *Sep. Purif. Technol.* 300 (2022) 121828. <https://doi.org/10.1016/j.seppur.2022.121828>.
- [63] J.K. Das, N. Das, S. Bandyopadhyay, Highly oriented improved SAPO 34 membrane on low cost support for hydrogen gas separation, *J. Mater. Chem. A* 1 (2013) 4966. <https://doi.org/10.1039/c3ta01095c>.
- [64] Z. Deng, M. Pera-Titus, In situ crystallization of b-oriented MFI films on plane and curved substrates coated with a mesoporous silica layer, *Mater. Res. Bull.* 48 (2013) 1874–1880. <https://doi.org/10.1016/j.materresbull.2013.01.020>.
- [65] C. Chen, L. Meng, K. Tung, Y.S. Lin, Effect of substrate curvature on microstructure and gas permeability of hollow fiber MFI zeolite membranes, *AIChE J.* 64 (2018) 3419–3428. <https://doi.org/10.1002/aic.16197>.
- [66] M.-H. Zhu, Z.-H. Lu, I. Kumakiri, K. Tanaka, X.-S. Chen, H. Kita, Preparation and characterization of high water perm-selectivity ZSM-5 membrane without organic template, *J. Membr. Sci.* 415–416 (2012) 57–65. <https://doi.org/10.1016/j.memsci.2012.04.037>.
- [67] S.M. Lee, Y.H. Lee, J.R. Grace, A. Li, C.J. Lim, F. Fotovat, A. Schaadt, R.J. White, S.S. Kim, Gas permeation properties of NaA zeolite membranes: effect of silica source on hydrogel synthesis and layer thickness, *J. Porous Mater.* 26 (2019) 1121–1129. <https://doi.org/10.1007/s10934-018-0707-z>.
- [68] X. Zhang, D. Tang, G. Jiang, Synthesis of zeolite NaA at room temperature: The effect of synthesis parameters on crystal size and its size distribution, *Adv. Powder Technol.* 24 (2013) 689–696. <https://doi.org/10.1016/j.appt.2012.12.010>.
- [69] S.F. Alam, M.-Z. Kim, Y.J. Kim, A. ur Rehman, A. Devipriyanka, P. Sharma, J.-G. Yeo, J.-S. Lee, H. Kim, C.-H. Cho, A new seeding method, dry rolling applied to synthesize SAPO-34 zeolite membrane for nitrogen/methane separation, *J. Membr. Sci.* 602 (2020) 117825. <https://doi.org/10.1016/j.memsci.2020.117825>.
- [70] Y. Liu, X. Wang, Y. Zhang, Y. He, X. Gu, Scale-up of NaA zeolite membranes on α -Al₂O₃ hollow fibers by a secondary growth method with vacuum seeding, *Chin. J. Chem. Eng.* 23 (2015) 1114–1122. <https://doi.org/10.1016/j.cjche.2015.04.006>.
- [71] K. Ueno, Y. Horiguchi, H. Negishi, M. Miyamoto, S. Uemiya, A. Takeno, Y. Sawada, Y. Oumi, Fabrication of high-performance silicalite-1 membrane by a novel seeding method using zeolite-dispersed polymer film, *Microporous Mesoporous Mater.* 261 (2018) 58–62. <https://doi.org/10.1016/j.micromeso.2017.11.001>.

- [72] L.S.M. Nazir, Y.F. Yeong, T.L. Chew, Methods and synthesis parameters affecting the formation of FAU type zeolite membrane and its separation performance: a review, *J. Asian Ceram. Soc.* 8 (2020) 553–571. <https://doi.org/10.1080/21870764.2020.1769816>.
- [73] L.S.M. Nazir, Y.F. Yeong, T.L. Chew, Study on the effect of seed particle size toward the formation of NaX zeolite membranes via vacuum-assisted seeding technique, *J. Asian Ceram. Soc.* 9 (2021) 586–597. <https://doi.org/10.1080/21870764.2021.1905252>.
- [74] Q. Wang, Y. Guo, N. Xu, Q. Liu, B. Wang, L. Fan, L. Zhang, R. Zhou, FAU zeolite membranes synthesized using nanoseeds — Separation mechanism and optimization for the pervaporation dehydration of various organic solvents, *J. Membr. Sci.* 696 (2024) 122522. <https://doi.org/10.1016/j.memsci.2024.122522>.
- [75] M. Ji, X. Gao, X. Wang, Y. Zhang, J. Jiang, X. Gu, An ensemble synthesis strategy for fabrication of hollow fiber T-type zeolite membrane modules, *J. Membr. Sci.* 563 (2018) 460–469. <https://doi.org/10.1016/j.memsci.2018.06.006>.
- [76] Z. Jabbari, S. Fatemi, M. Davoodpour, Comparative study of seeding methods; dip-coating, rubbing and EPD, in SAPO-34 thin film fabrication, *Adv. Powder Technol.* 25 (2014) 321–330. <https://doi.org/10.1016/j.appt.2013.05.011>.
- [77] M. Sakai, T. Kaneko, Y. Sasaki, M. Sekigawa, M. Matsukata, Formation Process of Columnar Grown (101)-Oriented Silicalite-1 Membrane and Its Separation Property for Xylene Isomer, *Crystals* 10 (2020) 949. <https://doi.org/10.3390/cryst10100949>.
- [78] H. Wang, Y.S. Lin, Effects of synthesis conditions on MFI zeolite membrane quality and catalytic cracking deposition modification results, *Microporous Mesoporous Mater.* 142 (2011) 481–488. <https://doi.org/10.1016/j.micromeso.2010.12.037>.
- [79] S. Askari, A. Bashardoust Siahmard, R. Halladj, S. Miari Alipour, Different techniques and their effective parameters in nano SAPO-34 synthesis: A review, *Powder Technol.* 301 (2016) 268–287. <https://doi.org/10.1016/j.powtec.2016.06.018>.
- [80] A. Nakhaei Pour, A. Mohammadi, Effects of Synthesis Parameters on Organic Template-Free Preparation of Zeolite Y, *J. Inorg. Organomet. Polym. Mater.* 31 (2021) 2501–2510. <https://doi.org/10.1007/s10904-021-01926-1>.
- [81] M. Jafari, A. Nouri, S.F. Mousavi, T. Mohammadi, M. Kazemimoghadam, Optimization of synthesis conditions for preparation of ceramic (A-type zeolite) membranes in dehydration of ethylene glycol, *Ceram. Int.* 39 (2013) 6971–6979. <https://doi.org/10.1016/j.ceramint.2013.02.034>.
- [82] B. Liu, H. Kita, K. Yogo, Preparation of Si-rich LTA zeolite membrane using organic template-free solution for methanol dehydration, *Sep. Purif. Technol.* 239 (2020) 116533. <https://doi.org/10.1016/j.seppur.2020.116533>.
- [83] M. Lee, S. Hong, D. Kim, E. Kim, K. Lim, J.C. Jung, H. Richter, J.-H. Moon, N. Choi, J. Nam, J. Choi, Chabazite-Type Zeolite Membranes for Effective CO₂ Separation: The Role of

- Hydrophobicity and Defect Structure, *ACS Appl. Mater. Interfaces* 11 (2019) 3946–3960. <https://doi.org/10.1021/acsami.8b18854>.
- [84] M.T. Conato, M.D. Oleksiak, B. Peter McGrail, R.K. Motkuri, J.D. Rimer, Framework stabilization of Si-rich LTA zeolite prepared in organic-free media, *Chem. Commun.* 51 (2015) 269–272. <https://doi.org/10.1039/C4CC07396G>.
- [85] H. Qiu, Y. Zhang, L. Kong, X. Kong, X. Tang, D. Meng, N. Xu, M. Wang, Y. Zhang, High performance SSZ-13 membranes prepared at low temperature, *J. Membr. Sci.* 603 (2020) 118023. <https://doi.org/10.1016/j.memsci.2020.118023>.
- [86] A. Simon, H. Richter, B. Reif, M. Schuelein, D. Sanwald, W. Schwieger, Evaluation of a method for micro-defect sealing in ZSM-5 zeolite membranes by chemical vapor deposition of carbon, *Sep. Purif. Technol.* 219 (2019) 180–185. <https://doi.org/10.1016/j.seppur.2019.03.017>.
- [87] G. Li, S. Fan, Z. Zhang, Y. Wang, X. Lang, J. Li, Mild ultraviolet detemplation of SAPO-34 zeolite membranes toward pore structure control and highly selective gas separation, *Sep. Purif. Technol.* 318 (2023) 123988. <https://doi.org/10.1016/j.seppur.2023.123988>.
- [88] B. Wang, C. Sun, R. Zhou, W. Xing, A super-permeable and highly-oriented SAPO-34 thin membrane prepared by a green gel-less method using high-aspect-ratio nanosheets for efficient CO₂ capture, *Chem. Eng. J.* 442 (2022) 136336. <https://doi.org/10.1016/j.cej.2022.136336>.
- [89] M. Zhou, L. Yu, J. Hedlund, Ultrathin DDR Films with Exceptionally High CO₂ Flux and Uniformly Adjustable Orientations, *Adv. Funct. Mater.* 32 (2022) 2112427. <https://doi.org/10.1002/adfm.202112427>.
- [90] M. Noack, M. Schneider, A. Dittmar, G. Georgi, J. Caro, The change of the unit cell dimension of different zeolite types by heating and its influence on supported membrane layers, *Microporous Mesoporous Mater.* 117 (2009) 10–21. <https://doi.org/10.1016/j.micromeso.2008.05.013>.
- [91] Y. Zhang, M. Wang, S. Liu, H. Qiu, M. Wang, N. Xu, L. Gao, Y. Zhang, Mild template removal of SAPO-34 zeolite membranes in wet ozone environment, *Sep. Purif. Technol.* 228 (2019) 115758. <https://doi.org/10.1016/j.seppur.2019.115758>.
- [92] S. Nai, X. Liu, W. Liu, B. Zhang, Ethanol recovery from its dilute aqueous solution using Fe-ZSM-5 membranes: Effect of defect size and surface hydrophobicity, *Microporous Mesoporous Mater.* 215 (2015) 46–50. <https://doi.org/10.1016/j.micromeso.2015.05.009>.
- [93] L. Donato, A. Garofalo, E. Drioli, O. Alharbi, S.A. Aljlil, A. Criscuoli, C. Algieri, Improved performance of vacuum membrane distillation in desalination with zeolite membranes, *Sep. Purif. Technol.* 237 (2020) 116376. <https://doi.org/10.1016/j.seppur.2019.116376>.
- [94] M. Lee, G. Lee, Y. Jeong, W.-J. Oh, J. Yeo, J.H. Lee, J. Choi, Understanding and improving the modular properties of high-performance SSZ-13 membranes for effective flue gas treatment, *J. Membr. Sci.* 646 (2022) 120246. <https://doi.org/10.1016/j.memsci.2021.120246>.

- [95] J. Kim, E. Jang, S. Hong, D. Kim, E. Kim, H. Richter, A. Simon, N. Choi, D. Korelskiy, S. Fouladvand, J. Nam, J. Choi, Microstructural control of a SSZ-13 zeolite film via rapid thermal processing, *J. Membr. Sci.* 591 (2019) 117342. <https://doi.org/10.1016/j.memsci.2019.117342>.
- [96] N. Chang, H. Tang, L. Bai, Y. Zhang, G. Zeng, Optimized rapid thermal processing for the template removal of SAPO-34 zeolite membranes, *J. Membr. Sci.* 552 (2018) 13–21. <https://doi.org/10.1016/j.memsci.2018.01.066>.
- [97] L. Wang, C. Zhang, X. Gao, L. Peng, J. Jiang, X. Gu, Preparation of defect-free DDR zeolite membranes by eliminating template with ozone at low temperature, *J. Membr. Sci.* 539 (2017) 152–160. <https://doi.org/10.1016/j.memsci.2017.06.004>.
- [98] L. Yu, D. Korelskiy, M. Grahn, J. Hedlund, Very high flux MFI membranes for alcohol recovery via pervaporation at high temperature and pressure, *Sep. Purif. Technol.* 153 (2015) 138–145. <https://doi.org/10.1016/j.seppur.2015.09.005>.
- [99] P. Kim, S. Hong, S.-E. Nam, Y.-I. Park, N. Choi, J.-H. Moon, J. Choi, On the effects of water exposure of as-synthesized LTA membranes on their structural properties and dehydration performances, *Sep. Purif. Technol.* 238 (2020) 116493. <https://doi.org/10.1016/j.seppur.2019.116493>.
- [100] Z. Chen, Y. Li, D. Yin, Y. Song, X. Ren, J. Lu, J. Yang, J. Wang, Microstructural optimization of mordenite membrane for pervaporation dehydration of acetic acid, *J. Membr. Sci.* 411–412 (2012) 182–192. <https://doi.org/10.1016/j.memsci.2012.04.030>.
- [101] J. Jiang, L. Peng, X. Wang, H. Qiu, M. Ji, X. Gu, Effect of Si/Al ratio in the framework on the pervaporation properties of hollow fiber CHA zeolite membranes, *Microporous Mesoporous Mater.* 273 (2019) 196–202. <https://doi.org/10.1016/j.micromeso.2018.07.015>.
- [102] W. Raza, J. Wang, J. Yang, T. Tsuru, Progress in pervaporation membranes for dehydration of acetic acid, *Sep. Purif. Technol.* 262 (2021) 118338. <https://doi.org/10.1016/j.seppur.2021.118338>.
- [103] Y. Hasegawa, T. Nagase, Y. Kiyozumi, T. Hanaoka, F. Mizukami, Influence of acid on the permeation properties of NaA-type zeolite membranes, *J. Membr. Sci.* 349 (2010) 189–194. <https://doi.org/10.1016/j.memsci.2009.11.052>.
- [104] S.M. Lee, N. Xu, J.R. Grace, A. Li, C.J. Lim, S.S. Kim, F. Fotovat, A. Schaadt, R.J. White, Structure, stability and permeation properties of NaA zeolite membranes for H₂O/H₂ and CH₃OH/H₂ separations, *J. Eur. Ceram. Soc.* 38 (2018) 211–219. <https://doi.org/10.1016/j.jeurceramsoc.2017.08.012>.
- [105] X.-L. Wei, S. Liang, Y.-Y. Xu, Y.-L. Sun, J.-F. An, Z.-S. Chao, Patching NaA zeolite membrane by adding methylcellulose into the synthesis gel, *J. Membr. Sci.* 530 (2017) 240–249. <https://doi.org/10.1016/j.memsci.2016.12.015>.
- [106] M. Xu, Y. He, Y. Wang, X. Cui, Preparation of a non-hydrothermal NaA zeolite membrane and defect elimination by vacuum-inhalation repair method, *Chem. Eng. Sci.* 158 (2017) 117–123. <https://doi.org/10.1016/j.ces.2016.10.001>.

- [107] D. Korelskiy, P. Ye, M.S. Nabavi, J. Hedlund, Selective blocking of grain boundary defects in high-flux zeolite membranes by coking, *J. Mater. Chem. A* 5 (2017) 7295–7299. <https://doi.org/10.1039/C7TA01268C>.
- [108] R. Zhou, H. Wang, B. Wang, X. Chen, S. Li, M. Yu, Defect-Patching of Zeolite Membranes by Surface Modification Using Siloxane Polymers for CO₂ Separation, *Ind. Eng. Chem. Res.* 54 (2015) 7516–7523. <https://doi.org/10.1021/acs.iecr.5b01034>.
- [109] Q. Dong, J. Jiang, S. Li, M. Yu, Molecular layer deposition (MLD) modified SSZ-13 membrane for greatly enhanced H₂ separation, *J. Membr. Sci.* 622 (2021) 119040. <https://doi.org/10.1016/j.memsci.2020.119040>.

Fig 1

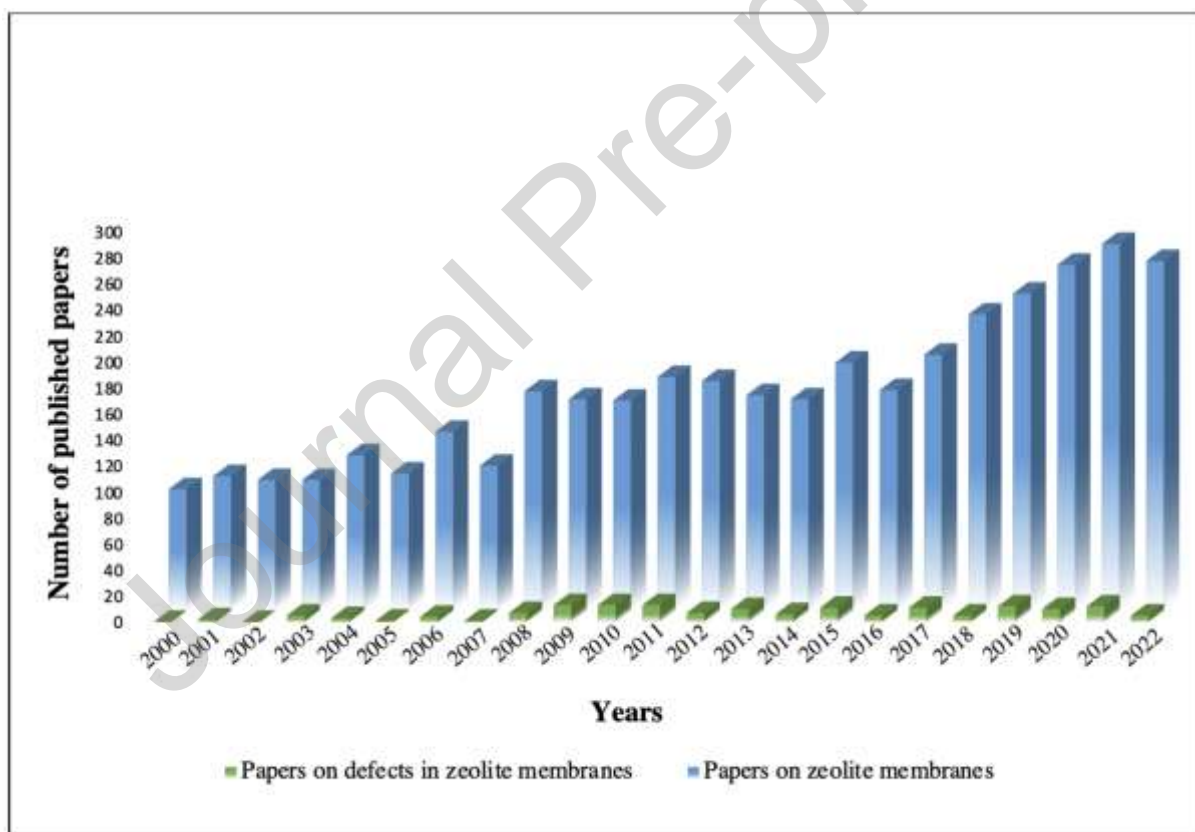


Fig 2

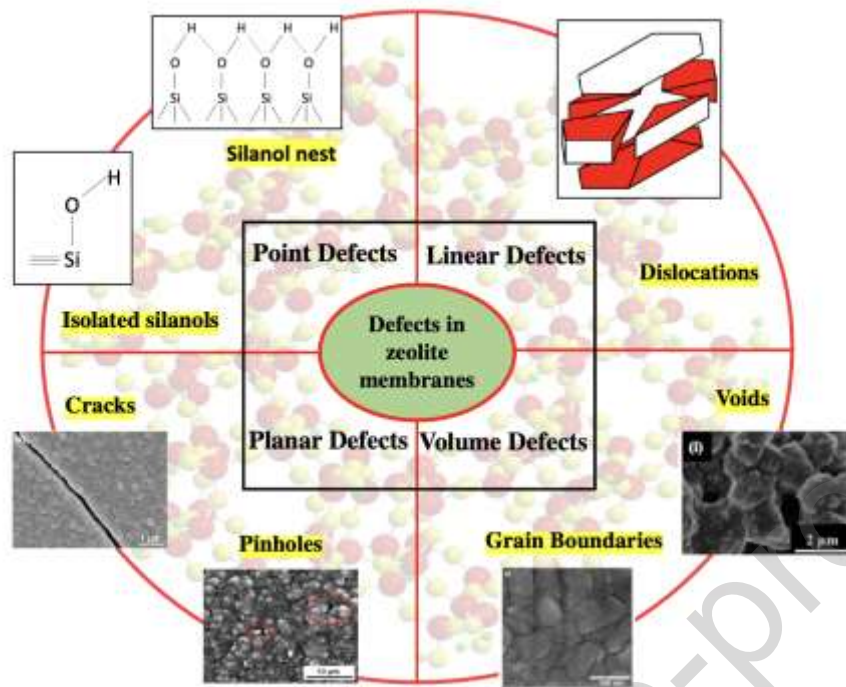


Fig 3

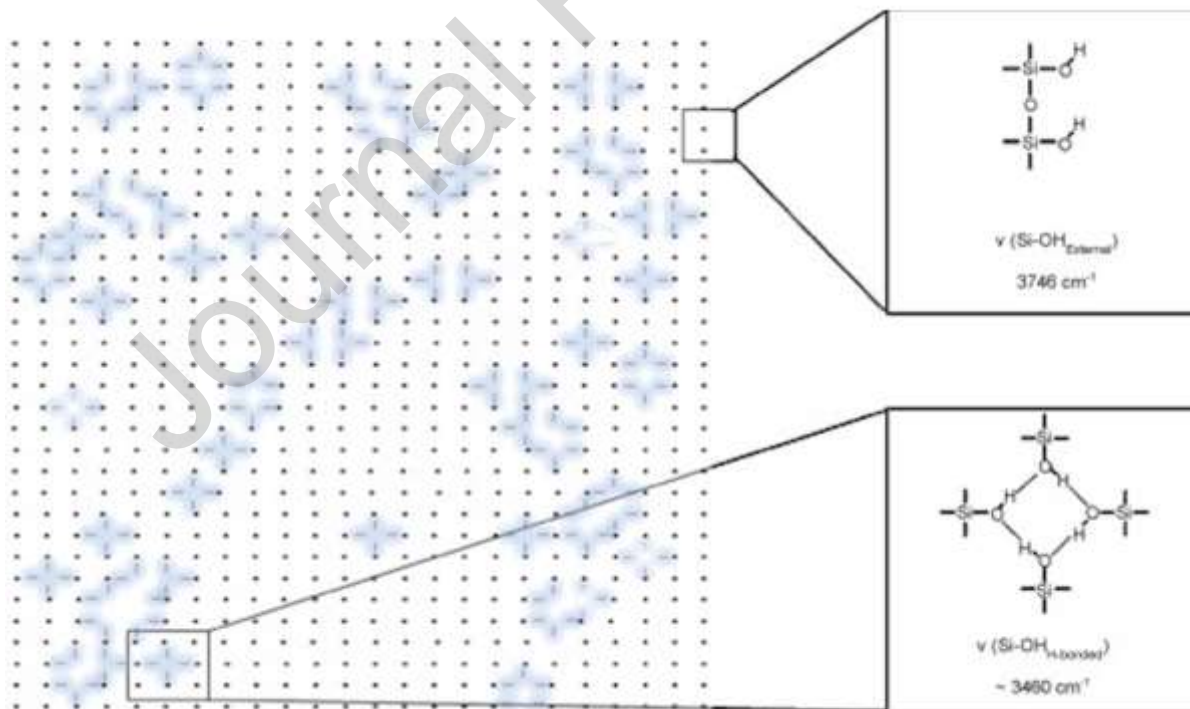


Fig 4

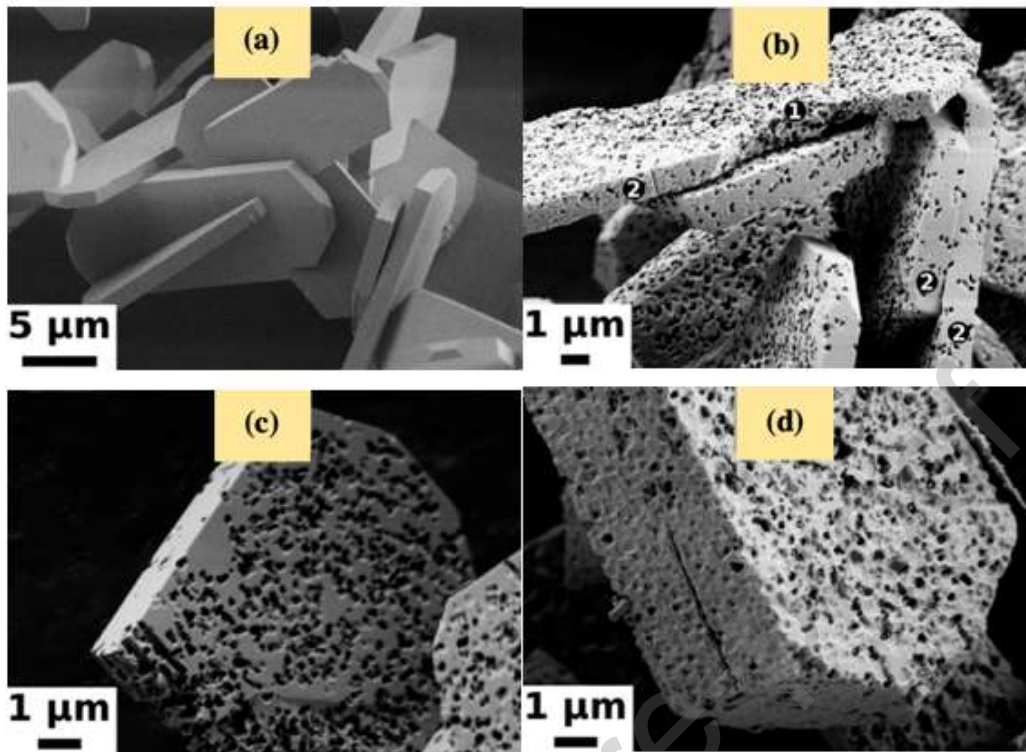


Fig 5

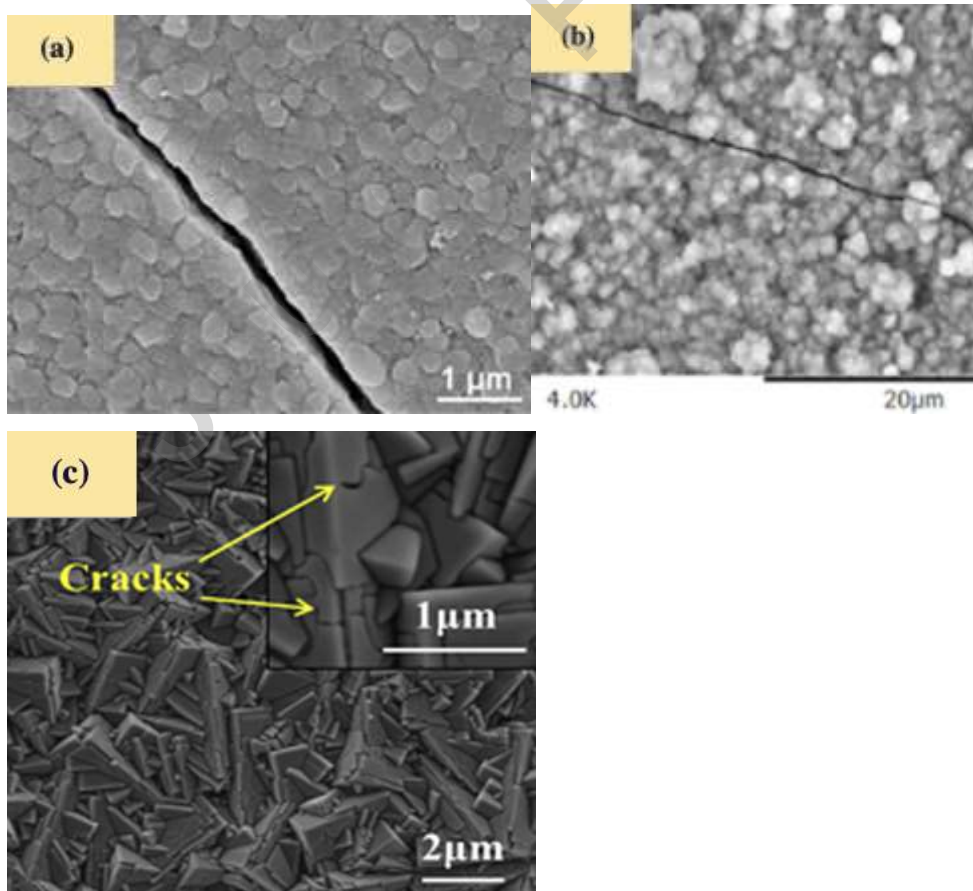


Fig 6

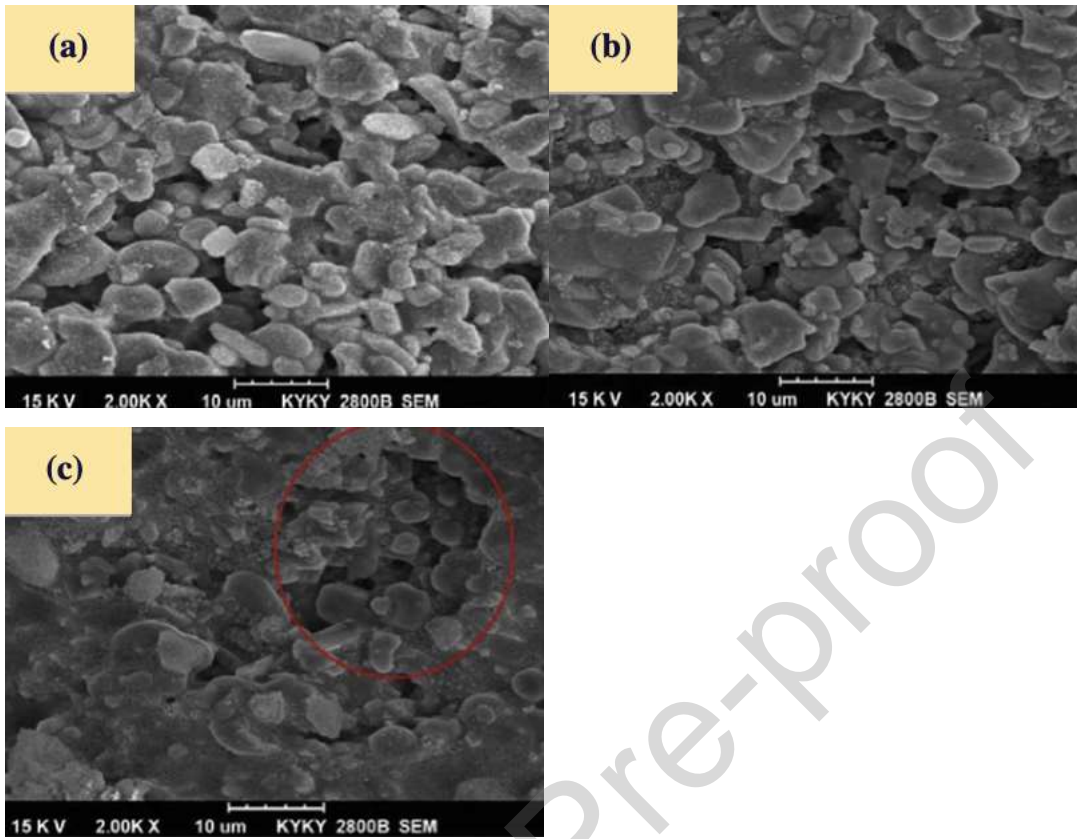


Fig 7

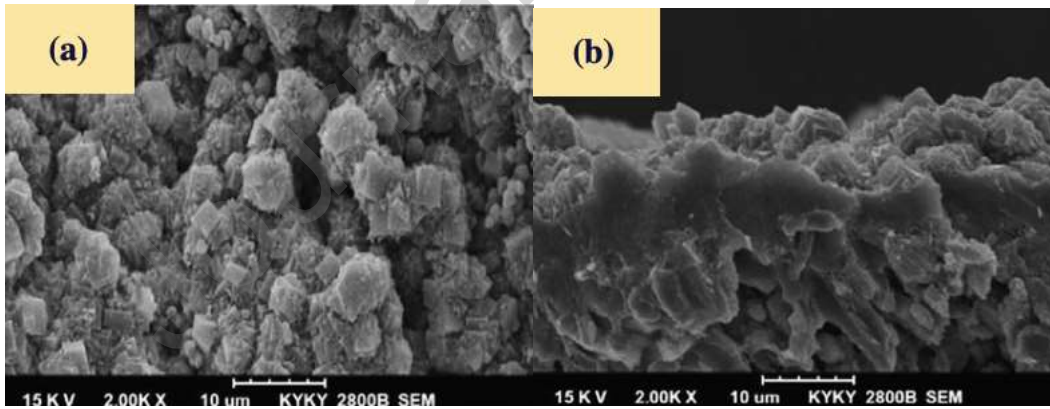


Fig 8

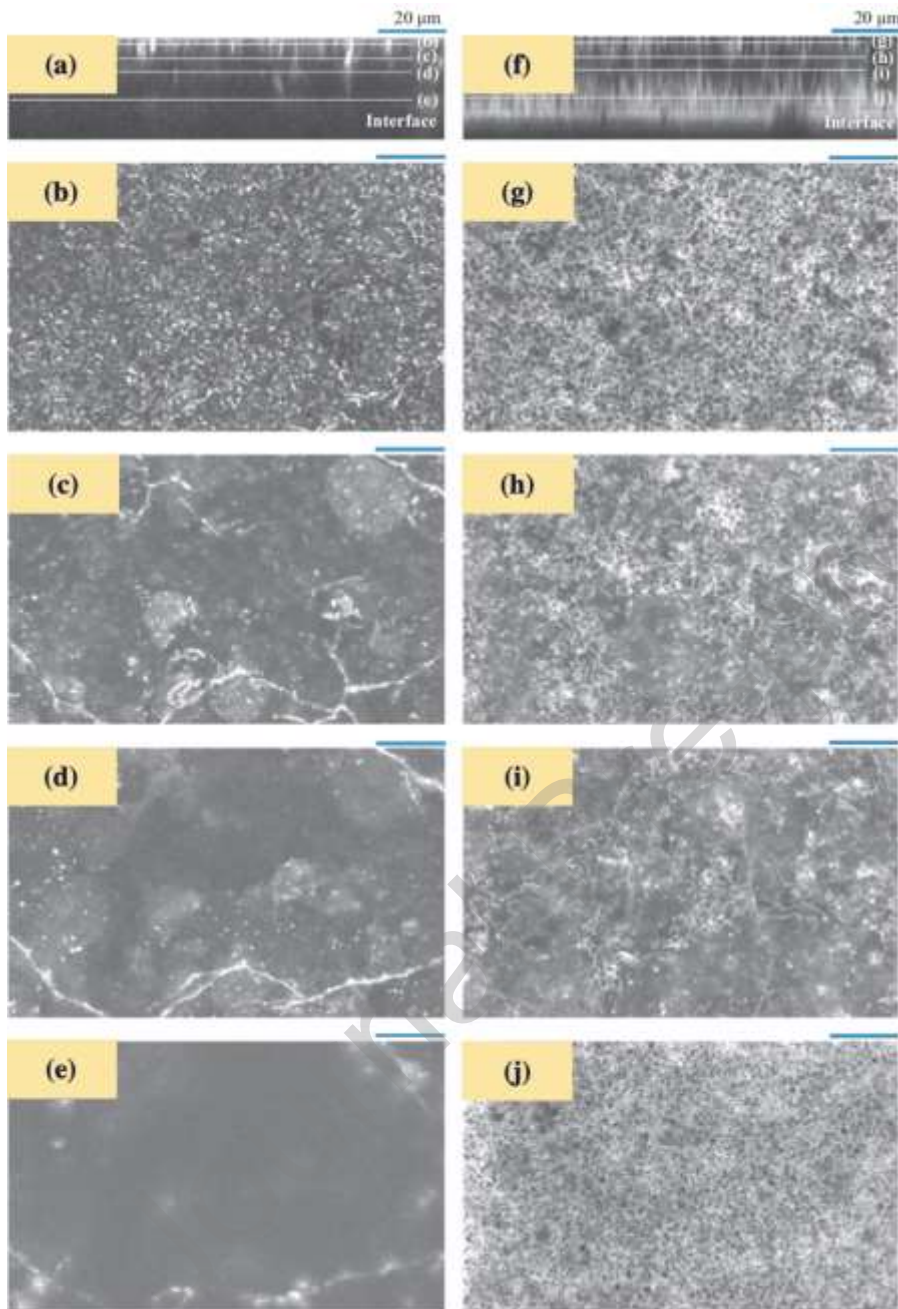


Fig 9

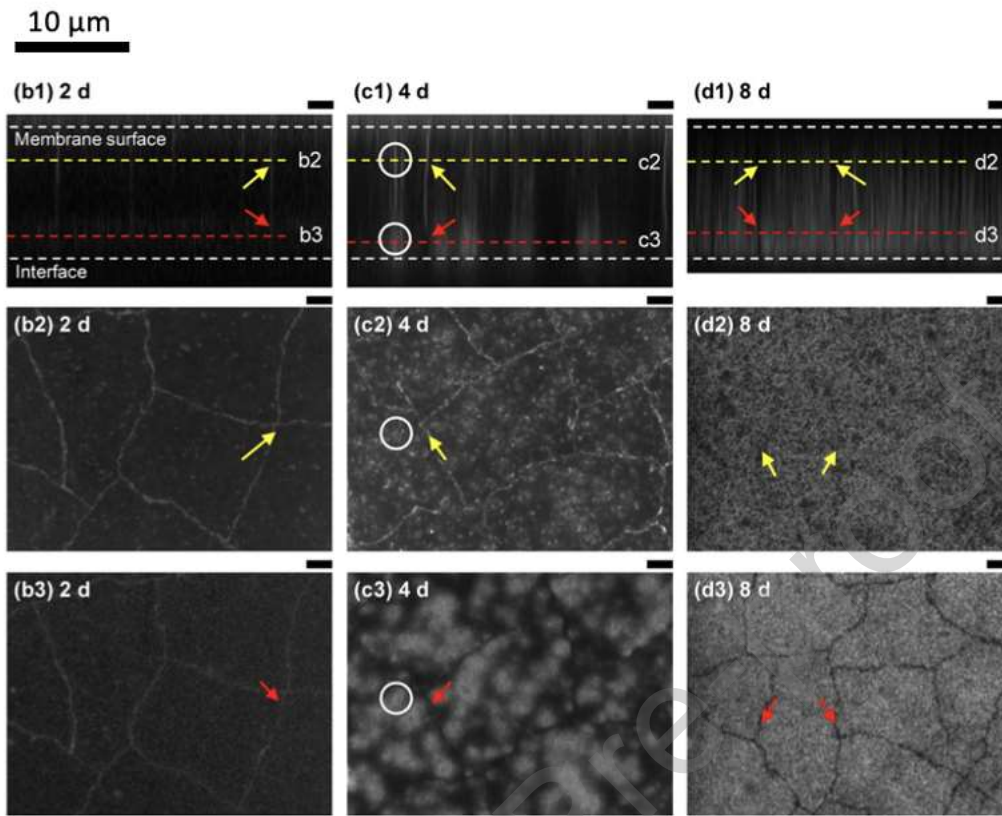
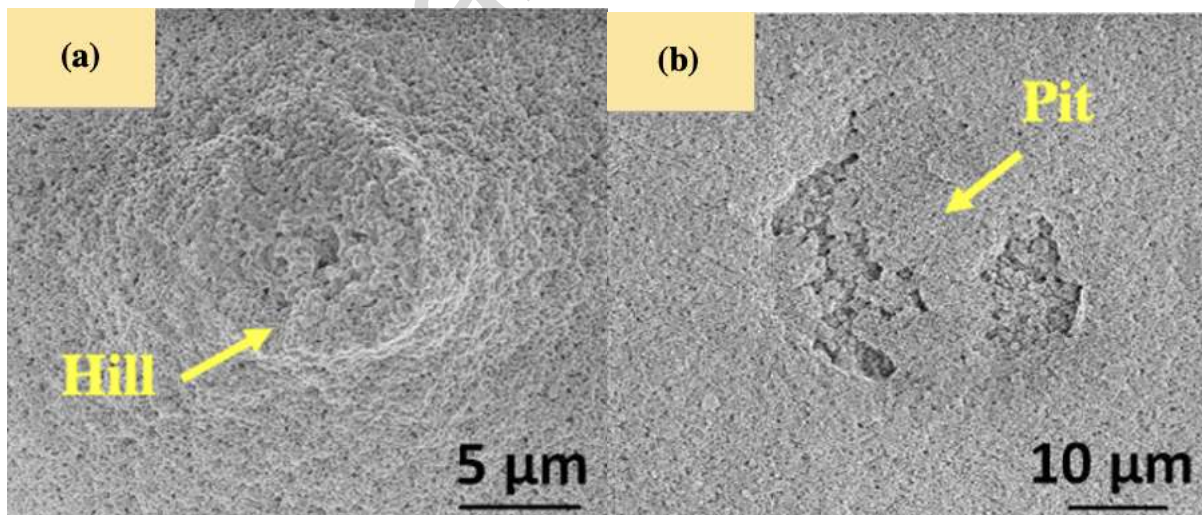


Fig 10



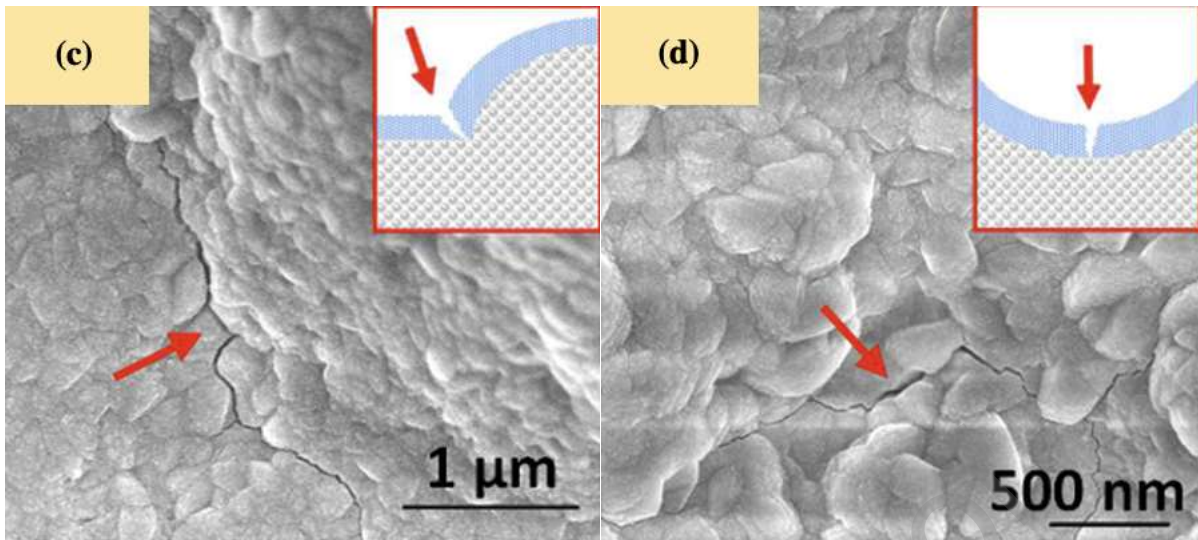


Fig 11

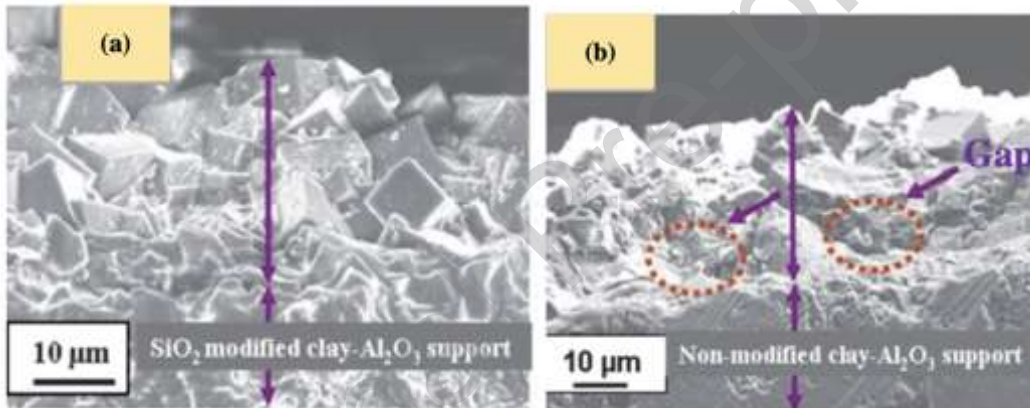


Fig 12

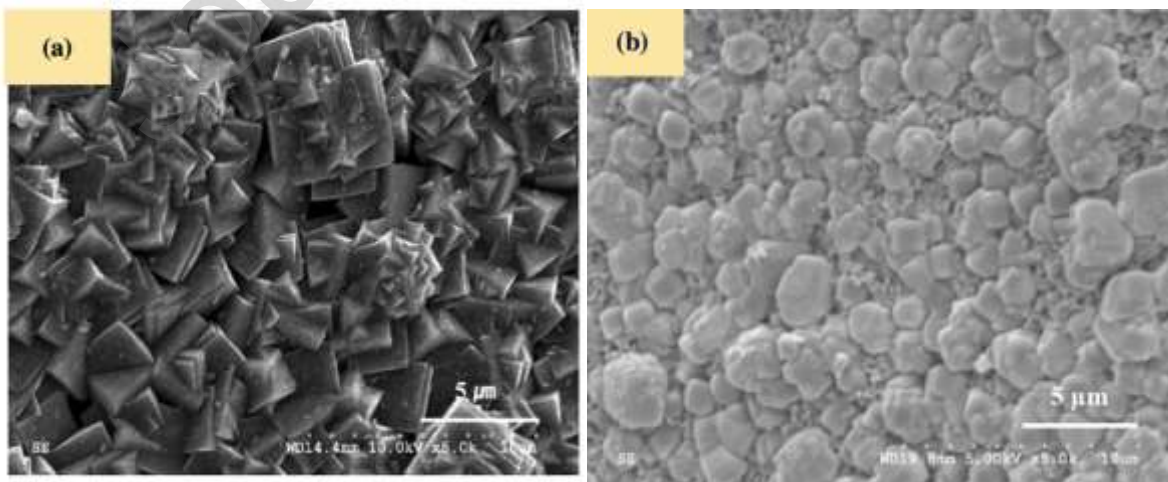


Fig 13

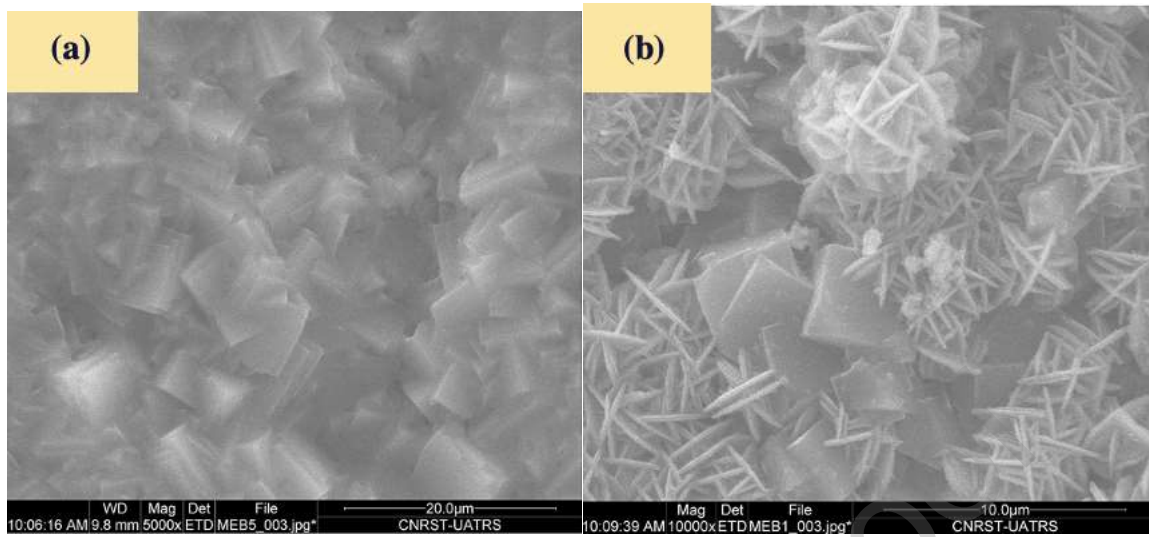


Fig 14

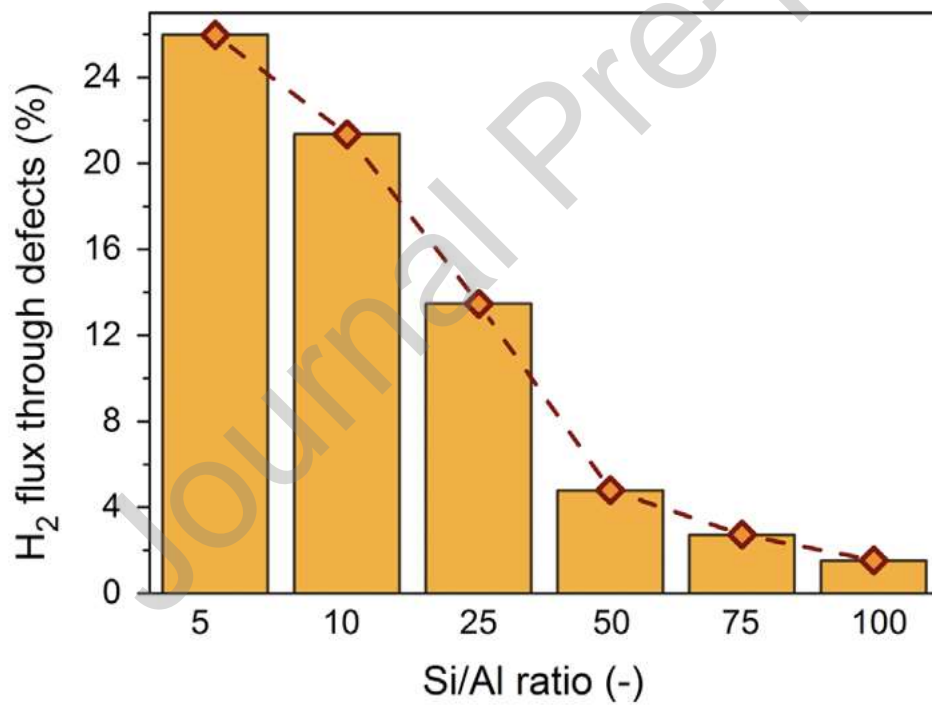


Fig 15

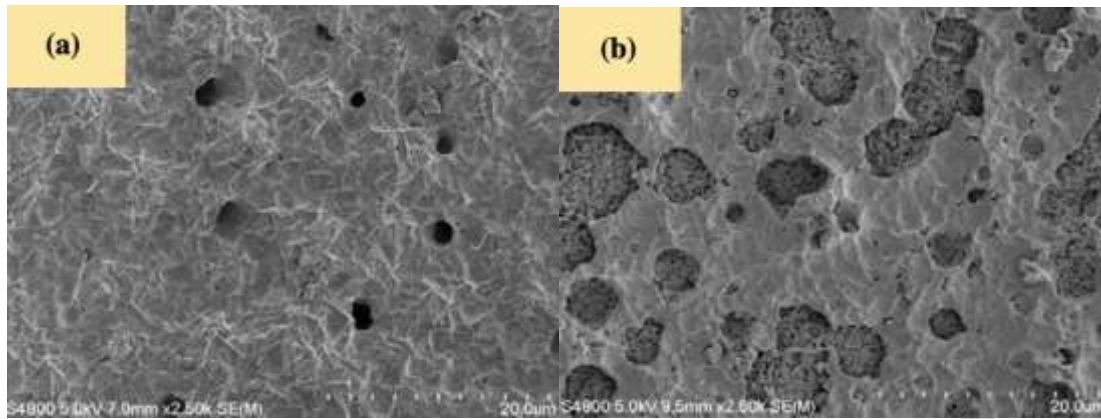


Fig 16

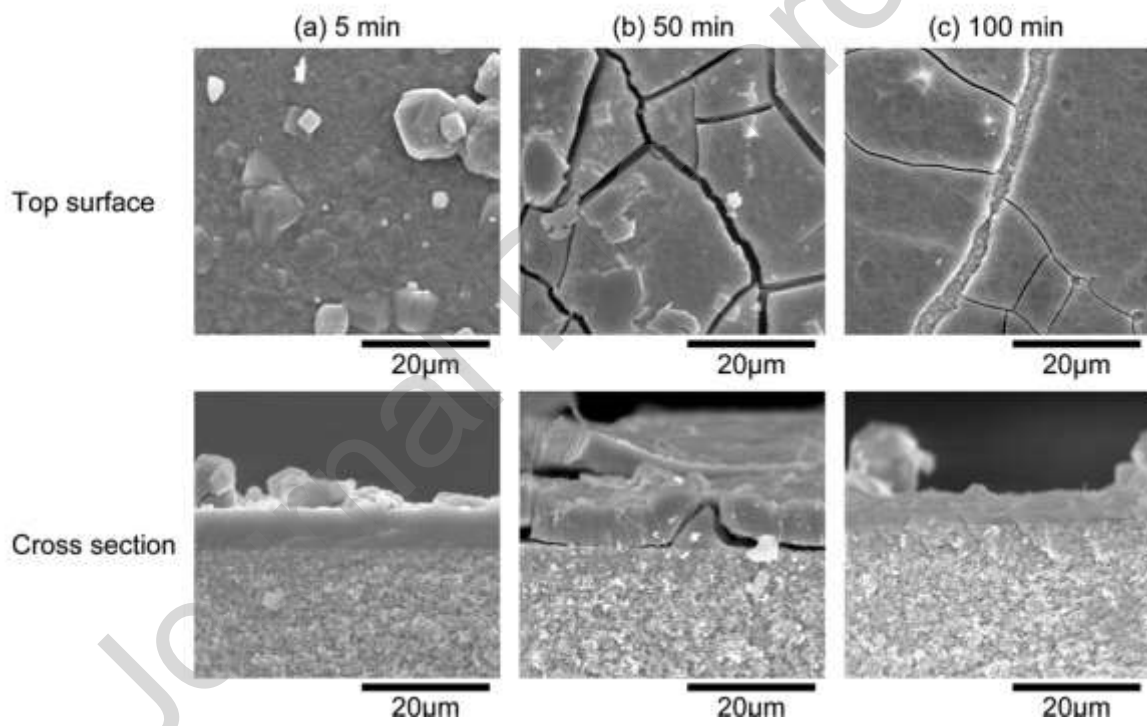


Fig 17

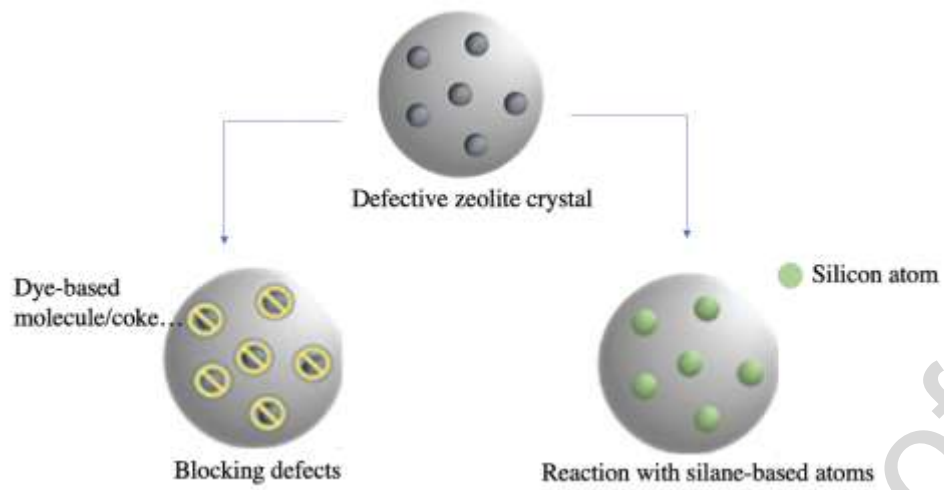
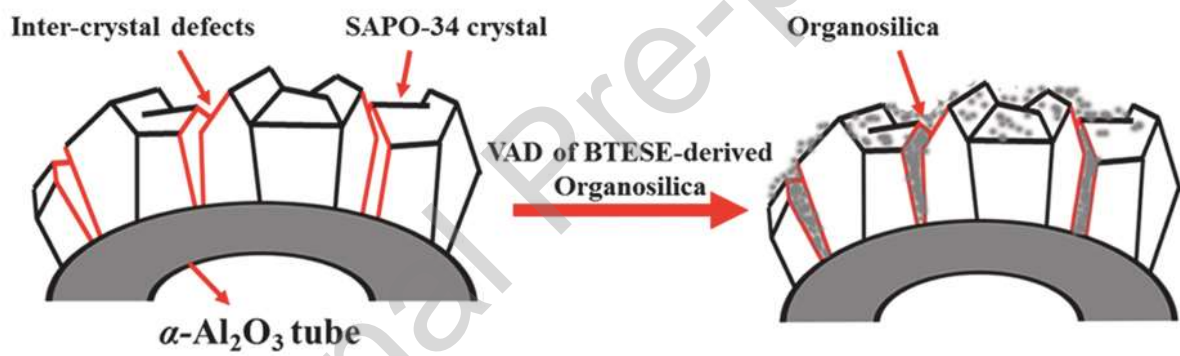


Fig 18



Graphical abstract

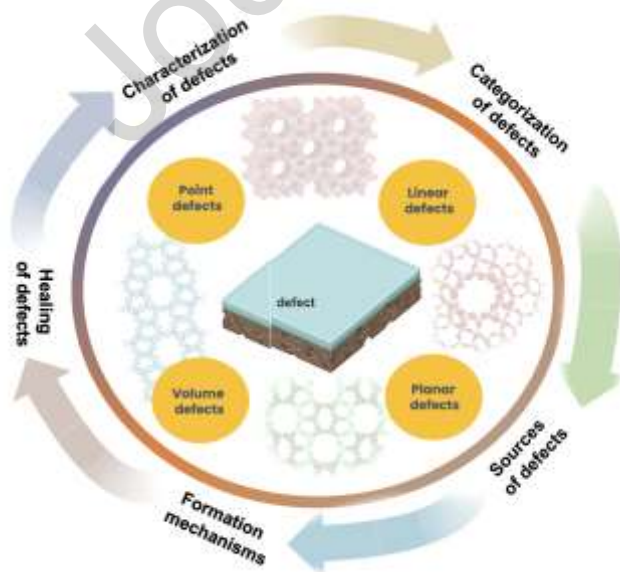


Table 1 Advantages and drawbacks of characterization techniques of defects.

	Technique	Advantages	Drawbacks
Direct techniques		- Non-destructive	
	SEM	- High resolution of images - No time consuming	- Limited to surface defects
			- Limited to thick membrane - Time consuming
	FCOM	- Non-destructive - 3D visualization of defect	- Low image resolution - Requires the use of a specific software to treat images
Indirect techniques	Gas permeation	- No specific equipment	- Unable to detect small variation in poorly defective membrane
			- Sensitive to the nature of the condensable component
	Permporosimetry	- Non-destructive - Simple operation - Practical for defects with a size less than 1 nm	- Adsorbed molecules may affect crystal size

Table 2 Seeding techniques of zeolite membranes.

Seeding technique	Zeolite type	Defect	Remarks	References
			- To increase the coverage zeolite layer, repeated coating cycles are necessary	
Dip-coating	NaY SAPO-34 Zeolite T	Pinholes	- Not appropriate for tubular substrates because of the impact of gravitation forces	[45,75,76]
Vacuum seeding	NaY	Cracks	- Long process - Rapid process - Thick layer - Easy process	[45]
Rub-coating	SAPO-34	Non-uniform layer	- Mechanical damage of zeolite seeds	[76]
Manual seeding	SAPO-34	Inhomogeneous layer	- Thick layer - Easy process - No specific equipment is required - Not reproducible	[69]

Table 3 Advantages and drawbacks of the cited template removal methods.

Method	Advantages	Drawbacks
Calcination	-High efficiency	-High energy consumption
	-Minimal chemical consumption	-Slow process: prolonged heating times
Rapid thermal processing	-Short processing time	-Requirement of many RTP cycles
Ozonication	-Reduced thermal stress	-Longer times of template removal

Table 4 Methods of reparation of defects in zeolite membranes.

Defect type	Zeolite membrane	source of defect	Proposed solution	Reference
Cracks	MFI	Support roughness	Polishing the support before membrane preparation	[58]
Cracks	SAPO-34	Calcination	VWD treatment	[44]
Cracks	SAPO-34	Calcination	VAD treatment	[14]
Intercrystal voids	SAPO-34	Lack of adherence between the support and zeolite film	Silica deposition at the surface of the support as an intermediate layer	[63]

Declaration of interest statement

The authors declare that they do not have any personal relationships or financial problems that could influence the work.

Highlights

- Reviewed direct and indirect characterizations of defects in zeolite membrane.
- Deeply discussed experimental factors generating defects in zeolite membranes.
- Reported specific healing techniques to deal with defects in zeolite membrane.
- Suggested future directions for preparing defect-free zeolite membranes.